Simplified derivation of the transfer function in dark matter models with relativistic corrections

Facultad de Ciencias - Máster en Astrofísica

Universidad de La Laguna

Tutor: Juan Betancort Rijo
Autora: Clara Iglesias Tesouro

Julio 2024

Abstract

A more advanced version (with respect to previous works [5]) of differential equations has been used to show the correct behavior, at all times $t > t_{hor}$, of the density fluctuations. In order to solve these equations, different numerical methods and approximations have been used. Through the analysis of the obtained solutions, a study is carried out on the main phenomena that affect density fluctuations, such as photon diffusion, Silk Damping, or free streaming. To illustrate the reliability of the solutions, different numerical analysis are made with the formalism used in [5], as well as qualitative comparisons with other publications [6]. Approximated relativistic corrections have been also implemented and studied, with the aim of describing the evolution of fluctuations at $t \lesssim t_{hor}$. Although the main objective has been to obtain relatively simple equations and their sufficiently precise solutions, the results also have practical interest. In particular, through immediate modifications, the effect of massive neutrinos or the possible decay of dark matter on the BAO can be determined.

Resumen

En el presente trabajo, se expone y resuelve numéricamente el sistema de ecuaciones diferenciales exactas (Betancort-Rijo 2024) que rigen la evolución de las fluctuaciones de densidad de fotones, bariones y materia oscura en el universo primordial. Este estudio surge como una continuación del trabajo previo [5], en el que se presentaban unas expresiones aproximadas cuyas soluciones describían correctamente el comportamiento de estas fluctuaciones hasta el momento del desacople. En este trabajo anterior, se trataba a los fotones y bariones como un único fluido casi-adiabático, al que se le añadía un factor correctivo para dar cuenta del efecto difusivo de los fotones durante las oscilaciones. Esta aproximación arrojaba buenos resultados, pero no es la interpretación correcta para la interacción radiación-materia. En el desarrollo de las nuevas ecuaciones tratadas en este trabajo, los fotones y bariones se consideran constituyentes independientes, cuyas fluctuaciones de densidad evolucionan cada una según una ecuación diferencial diferente, aunque simétrica. En cada una, se tiene en cuenta la interacción gravitatoria, el acoplamiento radiación-materia, la presión de radiación, las anisotropías en la distribución angular de fotones y la difusión de fotones que afectan a la evolución de ambas fluctuaciones, desde que la escala en cuestión entra en el horizonte hasta el momento del desacople, y que explican fenómenos importantes como el *Silk damping*.

Además, con este nuevo tratamiento, se logra reproducir también el comportamiento de las fluctuaciones más allá del momento del desacople, explicando el amortiguamiento de las fluctuaciones de radiación por el proceso de *free streaming* de fotones y el crecimiento de fluctuaciones bariónicas debido a la interacción gravitatoria.

En una segunda parte de este trabajo, se añaden las fluctuaciones de densidad correspondientes a la materia oscura, obteniendo también soluciones consistentes con el acelerado crecimiento bariónico que se sucede tras el desacople, causado por a la interacción gravi-

tatoria con la materia oscura. Con esta modificación, también se reproduce correctamente el continuo crecimiento de las perturbaciones de densidad de materia oscura, debido a que esta no interactúa electromagnéticamente con la materia bariónica ni con la radiación.

Por último, se consideran unas correcciones relativistas aproximadas, estrictamente necesarias para explicar el comportamiento de las fluctuaciones antes de su entrada en el horizonte, pues con el tratamiento relativista se obtiene un crecimiento erróneo de las perturbaciones. En este último análisis, se consideran también las fluctuaciones de densidad de neutrinos, para las que se obtienen unas soluciones cualitativamente correctas. Estas reflejan su comportamiento oscilatorio una vez la escala entra en el horizonte, similar al experimentado por los fotones, pero que únicamente es debido a la presión de los propios neutrinos.

Este trabajo se centra en la resolución numérica del nuevo sistema de ecuaciones, para la que serán necesarias diferentes aproximaciones, tanto teóricas como numéricas, y metodologías, con el objetivo de solventar inestabilidades en la integración y de ahorrar tiempo de cómputo. Para comprender cómo afectan cada una de las interacciones mencionadas a las fluctuaciones de densidad, se resuelve, en primer lugar, una versión parcial de las ecuaciones que tan solo considera la interacción gravitatoria, el acoplamiento radiación-materia y la presión de radiación. Posteriormente, se modifica esta expresión para dar cuenta de la anisotropía presente en la distribución angular de los fotones, efecto que disminuye la amortiguación de las oscilaciones. Por útlimo, se completan las ecuaciones con una serie de *términos de fuga de fotones*, que representan la difusión de fotones que provoca un mayor amortiguamiento de las oscilaciones, eliminándolas por completo en el caso de algunas escalas (*Silk damping*). Así, se consigue interpretar por separado la importancia de los diferentes efectos que influyen en la evolución de las fluctuaciones.

Una vez se tienen las ecuaciones completas y se han reproducido correctamente los diferentes efectos físicos que tienen lugar, se proponen dos metodologías para su resolución. Una primera aproximación, considerando una distribución exponencial del camino libre medio de los fotones a todo tiempo (que estrictamente sólo es válida para $t \lesssim t_{dec}$), arroja soluciones consistentes con trabajos anteriores, para los intervalos temporales analizados. Posteriormente, con una resolución más aproximada, mediante el método de Montecarlo, se obtienen soluciones que reproducen correctamente la evolución de las fluctuaciones de densidad más allá del desacople.

Se logra, así, obtener unas soluciones numéricas a las ecuaciones exactas, que describen adecuadamente los diferentes efectos e interacciones que tienen lugar entre los constituyentes del universo primordial, así como reproducen correctamente la evolución de sus fluctuaciones de densidad.

Contents

1 Introduction

Our universe is homogeneous and isotropic at large scale. This is the main hypothesis of modern cosmology, known as the first cosmological principle (1.1), and has been confirmed by multiple observations of the cosmic microwave background (CMB), such as those of COBE [3] or WMAP [12]. These observations (Figure 1) show that the temperature anisotropies at the recombination time were of the order of μK [9]. Moreover, the CMB is considered as the most perfect black-body, at the temperature $T = 2.725$ K [4], is the best fit ever obtained for the Planck distribution [7].

Despite this large-scale homogeneity, these small anisotropies are of special interest, as it is theorized [2] that these structures have grown over time, due to gravitational interaction, to become the galaxies and clusters we observe today. Such inhomogeneities can be treated as small-scale perturbations of a quasi-homogeneous and quasi-isotropic evolution of the large-scale universe. Thus, the problem can be approached using linear perturbation theory (1.2).

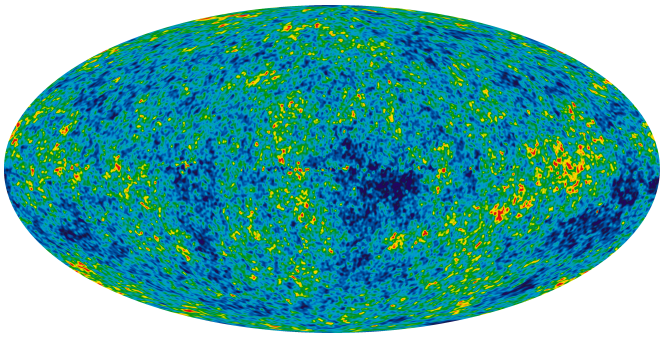

Figure 1: CMB anisotropies map, obtained from the weighted linear combination of the five WMAP frequency maps The linear scale goes from-200 to 200 µK. (NASA / LAMBDA Archive Team).

In this work, evolution equations of these density fluctuations (EEDF), obtained from a new exact formalism (Betancort Rijo, 2024) will be commented. Then their numerical solutions will be implemented and, through several approximations, the relevance of various physical effects are explored. Once these solutions have been obtained, they will be used to estimate different representative values of the composition of the universe throughout its evolution.

So, this work is structured as follows. In the remainder of this introduction, the cosmological principle and the universe of Friedmann-Robertson-Walker are presented in subsection 1.1 and linear perturbation theory is introduced in subsection 1.2. In section 2, we justify the motivations that have led us to develop this work, as well as provide the context for the research line, which has already been initiated in previous works [5], [1]. In section 3, we present the novel system of equations that describe the evolution of density fluctuations of

the different universe constituents. In section 4, several approximation methods and alternative procedures are presented, which were necessary to solve the equations correctly and avoid various instabilities. Finally, in section 5, we present the obtained results, considering a purely baryonic universe and also a universe with dark matter.

1.1 Cosmological principle and the Friedmann-Robertson-Walker universe

The universal homogeneity established by the cosmological principle implies that all observers in the universe see the same sequence of events. They can then synchronize their clocks to a *universal cosmic time*, t. This time can be identified with the universal Newtonian time. It can be shown [10] that the velocity $\vec{v}$ of any particle in the universe is either zero or positive directly proportional to the distance to the observer, $\vec{r}$.

$$\vec{v}(t) = H(t) \cdot \vec{r}(t) \tag{1}$$

Equation (1) explains Hubble's Law and hence $H(t)$ is known as the *Hubble's expansion parameter*. Writing $H(t) = \frac{\dot{a}(t)}{a(t)}$, this directly implies, integrating with time, that

$$\frac{d\vec{r}}{dt} = \frac{1}{a(t)}\frac{da(t)}{dt} \Rightarrow \vec{r}(t) = a(t) \cdot \vec{r}_0 \tag{2}$$

where $\vec{r}_0$ is a constant vector. That is, the expansion of the universe is spatially homogeneous and is governed by the so-called *scale factor* of the universe, $a(t)$. This spatial expansion affects the wavelength of radiation traveling through the universe, thus causing a *cosmological redshift*, z.

$$\frac{a(t)}{a_0} = \frac{1}{1+z} \tag{3}$$

being $a_0 \equiv a(t_0)$, that is, the scale factor at today's time, t_0. Given this definitions, the *Hubble constant* is defined as the Hubble's expansion parameter at $t = t_0$.

$$H_0 = \frac{\dot{a}_0}{a_0} \simeq 100 \text{ h}_0 \text{ km s}^{-1} \text{ Mpc}^{-1} \tag{4}$$

It can be shown [11] that the most general metric satisfying the cosmological principle previously stated is the *Robertson-Walker metric*.

$$ds^2 = -c^2dt^2 + a^2(t)\left[\frac{dr^2}{1-\varepsilon r^2} + r^2(sin^2\theta d\phi^2 + d\theta^2)\right] \tag{5}$$

where ε is the spatial curvature sign of the universe. This quantity can take the values $\varepsilon = \{0, \pm 1\}$. The case $\varepsilon = 0$ is that of an Euclidean space. $\varepsilon = +1$ and $\varepsilon = -1$ correspond to a spherical and hyperbolic geometric space, respectively. The metric of our universe (homogeneous and isotropic) is therefore determined by the curvature ε and the scale factor

$a(t)$.

The dynamics of a expanding universe are determined by the Einstein's field equation [11].

$$R^{\mu\nu} - \frac{1}{2}g^{\mu\nu}R = \frac{8\pi G}{c^4}T^{\mu\nu} \tag{6}$$

where $g^{\mu\nu}$ designates the metric, $T^{\mu\nu}$ is the energy-momentum tensor and $R^{\mu\nu}$ and R are the Ricci's tensor and scalar, respectively. Considering the case of a homogeneous and isotropic universe, the energy-momentum tensor takes the form of a perfect fluid, and the metric is as described above (5). In this framework, Einstein's equation field become a system of two second-order differential equations called *Friedmann's equations*.

$$\frac{\ddot{a}}{a} = -\frac{4\pi G}{3}\left(\rho + \frac{3p}{c^2}\right) \tag{7}$$

$$\left(\frac{\dot{a}}{a}\right)^2 = H^2 = \frac{8\pi}{3}\rho - \frac{\varepsilon}{a^2}c^2 \tag{8}$$

The system of Friedmann equations, together with a suitable *state equation*, $p = p(\rho)$, allows us to find the time evolution of the scale factor $a(t)$. For each component of the universe, the equation of state can be stated as a linear relation between pressure and density.

$$p = w\rho c^2 \tag{9}$$

The proportionality constant, w, takes different values depending on which constituent is considered (matter, radiation, curvature...). Assuming thermodynamic equilibrium among all the constituents of the universe, a single equation of state can be taken, which, together with the Friedmann equations, gives the evolution of the density as a function of the scale factor.

$$\rho = \rho_0 \left(\frac{a_0}{a}\right)^{3(1+w)} \tag{10}$$

The ω values and the corresponding relationships between density and scale factor, depending on which constituent dominates in each epoch of the universe, are listed below.

$$\begin{aligned}
&\text{Universe dominated by non-relativistic matter} \Rightarrow w = 0,\ \rho \propto a^{-3} \\
&\text{Universe dominated by radiation (relativistic matter)} \Rightarrow w = 1/3,\ \rho \propto a^{-4} \\
&\text{Universe dominated by cosmological constant} \Rightarrow w = -1,\ \rho \propto a^{0} \\
&\text{Universe dominated by curvature} \Rightarrow w = -1/3,\ \rho \propto a^{-2}
\end{aligned} \tag{11}$$

During its first $4.2 \cdot 10^5$ years of life, the universe was hot and very dense, the photons were energetic enough to keep the protons and electrons separated, forming an ionized plasma. The universe was then dominated by radiation, so density was $\rho \propto a^{-4}$. Then, the universe cools down and the *recombination* of protons and electrons into neutral H atoms takes place. Photons do not interact with neutral H, so they decouple from baryons, and the universe

became dominated by matter, $\rho \propto a^{-3}$, which experiences only the force of gravity (which is practically the self-gravity of the matter itself, since that corresponding to the photons is negligible).

From (8), we can define the critical density, ρ_c, such that the universe curvature is zero (12).

$$\rho_c \equiv \frac{3H^2}{8\pi} \tag{12}$$

$$\Omega_i = \frac{\rho_i}{\rho_c} \qquad\qquad \Omega_{i,0} = \frac{\rho_{i,0}}{\rho_c} \tag{13}$$

This allows us to define the dimensionless density parameters (13), which, at the present time, are constants. With this, we can rewrite second Friedmann equation as (14).

$$H = H_0 \sqrt{\sum_i \Omega_{i,0} a^{-3(1+w)}} \tag{14}$$

1.2 Linear perturbation theory

Linear perturbation theory considers the *real universe* or *perturbed universe* as the result of applying small local density perturbations $\delta(\vec{x}, t)$ to an *ideal universe*. The ideal universe, which preserves the properties of homogeneity and isotropy, and therefore has constant density $\rho(t)$, is the Friedmann-Robertson-Walker universe described in 1.1, and remains valid at large scales.

A density perturbation at a certain comoving point in the universe, $\vec{x}$, at a time t, is defined as a deviation from the density of the ideal universe.

$$\delta(\vec{x}, t) = \frac{\rho(\vec{x}, t) - \overline{\rho}(t)}{\overline{\rho}(t)} \ll 1 \tag{15}$$

In this linear regime, the growth of the perturbation δ is independent of its shape, so it is convenient to consider a spherical perturbation, which can be solved analytically, using the classical Newtonian theory of fluids. Applying then Euler, Poisson and continuity equations to this model, the second order differential equation (16) is obtained.

$$\ddot{\delta}_k + 2\frac{\dot{a}}{a}\dot{\delta}_k = 4\pi G\rho\delta_k - \frac{c_s^2 k^2}{a^2}\delta_k \tag{16}$$

Where we have considered the Fourier transformation of the density fluctuation (17), and $\vec{k}$ is its wavelength number ($\lambda = 2\pi/k$).

$$\delta_k = \frac{1}{(2\pi)^{3/2}} \int \delta(\vec{x}) e^{-i\vec{k}\cdot\vec{x}} d^n\vec{x} \tag{17}$$

First summand in equation 16 accounts for the gravitational attraction, which favors the growth of the fluctuation, while second represents radiation pressure, which opposes the former. If the term $\left(4\pi G\rho - \frac{c_s^2 k^2}{a^2}\right)$ is negative, equation 16 is the equation of a harmonic oscillator with variable amplitude (due to expansion): pressure gradient countereacts gravity and the amplitude of the fluctuation oscillates with time, mantaining a *stable regime* until radiation and baryonic matter decouple (*decoupling time*, t_{dec}). In the other case, where this term is positive, we have an *unstable regime*: gravity dominates and collapses the fluctuation. Thus, ***Jean's scale*** (18), is defined as the stability limit of density fluctuations. Scales such that $\lambda > \lambda_J$ will be unstable; gravity will be greater than the pressure gradient and fluctuations will grow, leading to the formation of structures.

$$\lambda_J = \frac{c_s}{a}\sqrt{\frac{\pi}{G\rho}} \tag{18}$$

From its expression, 18, dependent on the scale factor and the fluctuation density, it is clear that the *Jeans scale* varies with the expansion of the universe. Also, ***Jean's mass*** is defined as the mass enclosed in a sphere of radius λ_J.

In the *stable regime*, oscillations of density fluctuations give rise to zones of "overdensity", with higher temperature and energy, and zones of "underdensity", with lower temperature and energy. Thus, photon diffusion must take place, from denser to less dense zones. This effect would cause an additional damping of the oscillations, called ***Silk damping*** or diffusion damping. This damping may be such that it completely eliminates the oscillation before decoupling occurs. ***Silk's scale*** is then defined, such that scales with $M < M_{Silk}$ will be damped out.

$$M_{Silk} = 1.3 \cdot 10^{12} \cdot (\Omega_{0,bar} h^2)^{-3/2}\ M_\odot \tag{19}$$

M_{Silk} is defined so that the damping is a factor $1/e$, which, in a pure baryonic universe, takes the value (19) [8].

2 Motivations and theoretical context

In previous works, [5], [1], approximate equations of evolution of density fluctuations were obtained in such a way that they explained well the behavior of the density fluctuations, from instants immediately after inflation, up to the decoupling between radiation and baryonic matter. The aim of this work is to find a single system of formally exact equations, whose solutions describe the evolution of the fluctuations at any instant of time after inflation, both before and after decoupling. The reliability of this new equations, already consistent by construction, will be demonstrated through the study of their numerical solutions, which will form the central framework of this work.

In [5], the evolution of photon and baryon fluctuations (δ_γ and δ_{bar}, respectively) was approximated by treating them as a single fluid, in which both components were strongly

coupled. It was considered, then, a single second order differential equation for baryon fluctuations, along with a simple first-order differential equation (20) to obtain photon fluctuations, that account for photon leakage.

$$\dot{\delta}_\gamma = \frac{4}{3}\dot{\delta}_{bar} - \frac{\vec{\nabla}_x \cdot \vec{F}_\gamma}{\rho_\gamma} \tag{20}$$

This equation is a quasi-adiabatic relation between baryons and photons, modified by the photon flux, $\vec{F}_\gamma$, in the comoving system with baryons. Photon flux is given by $\vec{F}_\gamma = -\mu\rho_\gamma\vec{\nabla}_x\delta_\gamma$, where μ is the coefficient of photon energy diffusion, $\mu = \frac{1}{3}\frac{1}{n_e(a)\sigma_T}c$, given by the mean free path approach of the kinetic theory. Relation (20) can also be expressed in transformed Fourier space as (21).

$$\dot{\delta}_{\gamma,k} = \frac{4}{3}\dot{\delta}_{bar} - \mu\frac{k^2}{a^2}\delta_{\gamma,k} \tag{21}$$

This approximation, based on classical fluid mechanics, is valid as long as the photon mean free path, $\bar{\lambda} = 1/n_e\sigma_T$, is small compared to the considered scale length, λ, which holds true for relevant scales up to previous instants close to decoupling. This has been a suitable approximation for treating Silk damping, but if we wanted to apply it to obtain the dark matter transfer function, or more generally, to obtain the evolution of fluctuations δ_{bar}, δ_γ and δ_{DM} during and beyond decoupling, we would need to consider photons and baryons as two separate fluids, coupled only by gravity. This would lead to a sudden change in regime at the decoupling moment, transitioning from the single-fluid treatment to the two-fluid treatment.

A standard treatment of the problem involves the application of kinetic theory (Boltzmann equation for statistical equilibrium), which leads to complex integro-differential equations. However, in the present work, a different approach (Betancort-Rijo, 2024) is proposed, which allows obtaining a system of second-order differential equations for δ_{bar}, δ_γ and δ_{DM}. These equations are formally exact, although some approximations are applied, with negligible errors, solely motivated by simplifying their numerical resolution and saving computational cost. As mentioned earlier, in this approach, photons and baryons each follow a different second-order differential equation. Photons experience gravity and the associated pressure, as well as deceleration (during the decreasing phase) or acceleration (during the increasing phase) caused by baryons through Thomson scattering. On the other hand, baryons only experience the force of gravity and the drag caused by photons.

The velocity of a *photonic fluid element* is determined by the velocity of the reference frame in which the average momentum of photons is zero. This velocity is given by the action of gravity and the pressure gradient. The displacement divergence, up to a given time, determines the δ_γ at that time. But, in addition to this evolution of δ_γ due to the fluid elements motions, the gradient of photon number density, n_γ, implies an additional flow of photons (and, therefore, of their associated energy) in the proper frame with these elements. This

leads to the inclusion of additional terms, called *"photon leakage terms"* in the evolution equation for δ_γ.

If $\bar{\lambda} \ll \lambda$[1], when the single-fluid treatment of [5] is valid, the *photon pressure term* considered in this work coincides with that of [5]. However, when $\bar{\lambda} \lesssim \lambda$, this pressure term is modulated by a certain function of $k\bar{\lambda}$, which is smaller, in absolute value, than in [5]. This is because, in this limit, photon angular distribution is no longer isotropic. The effect of this anisotropy is determined by the function $G(k\lambda_0)$ given by an an interpolating fit (8), for photons that have traveled freely a comoving distance λ_0 (22) since their last scattering, at time t_e.

$$\lambda_0(t_e, t) = \int_{t_e}^{t} \frac{c}{a(t')} dt' \tag{22}$$

To obtain the exact pressure term, one must average $G(k\lambda_0)$ over the probability distribution of λ_0, with mean $\bar{\lambda}$, at each given time t (23).

$$\langle G(k\lambda_0)\rangle(t) = \int_0^t G\left(k\lambda_0\left(t_e, t\right)\right) P_t(t_e) dt_e \tag{23}$$

where $P_t(t_e)$ is the probability distribution of the time of last scattering, t_e, before time t.

$$P_t(t_e) = e^{-\tau(t_e,t)} \sigma_T n_e(t_e) c \tag{24}$$

given the optical depth from t_e to t:

$$\tau(t_e, t) = \int_{t_e}^{t} \sigma_T n_e(t') c dt' \tag{25}$$

The same occurs with photon leakage terms, which are proportional to the average (27) of a function $V(k\lambda_0)$, given by (26).

$$V(y) = \frac{\sin(y) - y\cos(y)}{y^2} \tag{26}$$

$$\langle V(k\lambda_0)\rangle(t) = \int_0^t V\left(k\lambda_0\left(t_e, t\right)\right) P_t(t_e) dt_e \tag{27}$$

Until times shortly after decoupling, the probability distribution of λ_0 is exponential, and therefore the averaging in (23) and (27) can be performed analytically, using $H(k\bar{\lambda})$, specified in (28).

$$H(k\bar{\lambda}) = \int_0^{\inf} e^{-\lambda_0/\bar{\lambda}} G(k\lambda_0) d\lambda_0 \tag{28}$$

$$\langle G(k\lambda_0)\rangle = H(k\bar{\lambda}) \quad \text{if} \quad t < t_{dec} \tag{29}$$

[1] As mentioned earlier, and as will remain throughout this work, $\bar{\lambda}$ denotes the mean free path, and λ is the mode wavelength.

$$\langle V(k\lambda_0)\rangle = k\bar{\lambda}H(k\bar{\lambda}) \quad \text{if} \quad t < t_{dec} \tag{30}$$

However, for times long after decoupling, although λ_0, is similar for all photons, the function $G(k\lambda_0)$ changes significantly with λ_0. For this reason, neither $H(k\bar{\lambda})$ nor $G(k\bar{\lambda})$ can be used and, instead, it is necessary to average with the exact probability distribution, which is no longer exponential. This makes the treatment more complicated (further explained later in this work).

It should also be mentioned that the equations used in this work lead to an initial growth (at times $t \lesssim t_{hor}$) of the fluctuations that is not correct. At times before the scale enters the horizon, certain relativistic corrections must be applied, which will also be presented as the final part of this work.

3 Novel equations of evolution of density fluctuations

With the approach mentioned in the previous section (Betancort-Rijo, 2024), the following equations are obtained for the evolution of density fluctuations of photons δ_γ, baryons, δ_{bar}, and dark matter, δ_{DM}.

$$\ddot{\delta}_{k,\gamma} + 2\frac{\dot{a}}{a}\dot{\delta}_{k,\gamma} = \underbrace{\frac{16}{3}\pi G\left(\rho_{bar}\delta_{k,bar} + 2\rho_\gamma\delta_{k,\gamma} + \rho_{DM}\delta_{k,DM}\right)}_{\text{gravitational interaction}} + \underbrace{\frac{7}{12}\sigma_T n_e c\left(\dot{\delta}_{k,bar} - \frac{3}{4}\dot{\delta}_{k,\gamma}\right)}_{\text{photon-baryon coupling}}$$
$$\underbrace{-\frac{k^2}{a^2}c^2\langle G(k\lambda_0)\rangle\delta_{k,\gamma}}_{\text{photon pressure}} \underbrace{-\frac{\dot{a}}{a}\frac{kc}{a}\langle V(k\lambda_0)\rangle - \frac{kc}{a}\langle V(k\lambda_0)\rangle\dot{\delta}_{k,\gamma} - \frac{k^2c}{a}\langle G(k\lambda_0)\rangle\dot{\bar{\lambda}}\delta_{k,\gamma}}_{\text{photon leakage}} \tag{31}$$

$$\ddot{\delta}_{bar} + 2\frac{\dot{a}}{a}\dot{\delta}_{bar} = \underbrace{4\pi G\left(\rho_{bar}\delta_{bar} + 2\rho_\gamma\delta_\gamma + \rho_{DM}\delta_{k,DM}\right)}_{\text{gravitational interaction}} - \underbrace{\frac{7}{12}\sigma_T n_e c\frac{\rho_\gamma}{\rho_{bar}}\left(\dot{\delta}_{bar} - \frac{3}{4}\dot{\delta}_\gamma\right)}_{\text{photon-baryon coupling}} \tag{32}$$

$$\ddot{\delta}_{DM} + 2\frac{\dot{a}}{a}\dot{\delta}_{DM} = \underbrace{4\pi G\left(\rho_{bar}\delta_{bar} + 2\rho_\gamma\delta_\gamma + \rho_{DM}\delta_{k,DM}\right)}_{\text{gravitational interaction}} \tag{33}$$

With $\langle G(k\lambda_0)\rangle$ and $\langle V(k\lambda_0)\rangle$ given by (23) and (27). The integration of this equations, along with suitable initial conditions, gives us the evolution of the density fluctuations. As the main interest is the relative value of the fluctuations at each time, we chose the initial conditions (34), corresponding to the increasing mode.

$$\delta_\gamma(t_{in}) = \frac{4}{3} \qquad \dot{\delta}_\gamma(t_{in}) = \frac{4}{3}\frac{1}{t_{in}} \qquad \delta_{DM}(t_{in}) = \delta_{bar}(t_{in}) = 1 \qquad \dot{\delta}_{bar}(t_{in}) = \dot{\delta}_{DM}(t_{in}) = \frac{1}{t_{in}} \tag{34}$$

Energy densities of each constituent, ρ_{bar}, ρ_γ, ρ_{DM}, can be calculated according to (35), (36), (37), obtained from (10) and the definition of dimensionless density parameter at the present time, $\Omega_{i,0} \equiv \rho_{i,0}/\rho_{i,c}$.

$$\frac{\rho_{bar}(t)}{\rho_t(t)} = \frac{\Omega_{0,bar}a^{-3}}{(\Omega_{0,DM}+\Omega_{0,bar})a^{-3}+\Omega_{0,rad}a^{-4}} \tag{35}$$

$$\frac{\rho_{DM}(t)}{\rho_t(t)} = \frac{\Omega_{0,DM}a^{-3}}{(\Omega_{0,DM}+\Omega_{0,bar})a^{-3}+\Omega_{0,rad}a^{-4}} \tag{36}$$

$$\frac{\rho_\gamma(t)}{\rho_t(t)} = \frac{\Omega_{0,\gamma}a^{-4}}{(\Omega_{0,DM}+\Omega_{0,bar})a^{-3}+\Omega_{0,rad}a^{-4}} \tag{37}$$

The different terms, theoretically introduced in section 2, can be distinguished in equations (31), (32) and (33). In all three equations there is a **gravitational term** (first summand on the right-hand side), proportional to the gravitational constant G and to the density of all the constituents. This term is always positive, since it represents an attractive force that favors the increase of the fluctuation density.

The second summand on the right-hand side in (31) and (32), proportional to $\left(\dot{\delta}_{bar} - \frac{3}{4}\dot{\delta}_\gamma\right)$, accounts for the **coupling** between photons and baryons. This term is negative for photons in the decreasing phase, since baryons pull back photons that tend to escape from over-dense regions (the opposite happens to baryons). As mentioned above, in previous works [5], the set of photons and baryons was considered as a single quasi-adiabatic fluid, with a small modification to account for photon diffusion. In this work, photons and baryons are considered as two independent constituents from the beginning, interacting by gravity and Thomson scattering. This interaction is strongly dominant before decoupling, so photons and baryons will oscillate synchronously until this moment.

In (31), there are four additional terms. First one, proportional to the average of $G(k\lambda_0)$, is the relative to the **photon-photon pressure**, previously mentioned. This term accounts for the decrease in photon density due to intrinsic collisions between photons. Last three terms are the defined **"photon leakage terms"**.

Once this equations have been presented, the next step is to solve them and analyze their solutions. As mentioned, this differential system has no analytical solution, so numerical integration methods have been used to solve the system simultaneously with Friedmann equation (14).

4 Numerical resolution: Methodology and instabilities

Direct numerical integration of equations (31) and (32) gives rise to an instability, caused by the strong coupling between photons and baryons. Slight differences in $\dot{\delta}_\gamma$ and $\dot{\delta}_{bar}$, resulting

from numerical errors, led to artificially large values of the coupling terms, which give rise to an instability. In order to avoid this instability, an alternative quantity is introduced: $\dot{\Delta} \equiv \dot{\delta}_{k,bar} - \frac{3}{4}\dot{\delta}_{k,\gamma}$. Taking equations (31) and (32), we derive (39) as the new differential equation for baryonic density fluctuations.

$$\ddot{\delta}_{k,\gamma} + 2\frac{\dot{a}}{a}\dot{\delta}_{k,\gamma} = \frac{16}{3}\pi G\left(\rho_{bar}\delta_{k,bar} + 2\rho_\gamma\delta_{k,\gamma} + 2\rho_{DM}\delta_{DM}\right) + \frac{7}{12}\sigma_T n_e c\dot{\Delta} - \frac{k^2}{a^2}c^2\langle G(k\lambda_0)\rangle\delta_{k,\gamma} - \frac{\dot{a}}{a}\frac{kc}{a}\langle V(k\lambda_0)\rangle - \frac{kc}{a}\langle V(k\lambda_0)\rangle\dot{\delta}_{k,\gamma} - \frac{k^2c}{a}\langle G(k\lambda_0)\rangle\dot{\bar{\lambda}}\delta_{k,\gamma} \quad (38)$$

$$\ddot{\Delta} + 2\frac{\dot{a}}{a}\dot{\Delta} = -\sigma_T n_e c\left(\frac{\rho_\gamma}{\rho_{bar}} + \frac{3}{4}\right)\dot{\Delta} + \frac{3k^2}{4a^2}c^2\delta_{k,\gamma}\langle G(k\lambda_0\rangle) + \frac{3}{4}\frac{\dot{a}}{a}\frac{kc}{a}\langle V(k\lambda_0)\rangle + \frac{3}{4}\frac{kc}{a}\langle V(k\lambda_0)\rangle\dot{\delta}_{k,\gamma} + \frac{3}{4}\frac{k^2c}{a}\langle G(k\lambda_0)\rangle\dot{\bar{\lambda}}\delta_{k,\gamma} \quad (39)$$

Despite this change of formalism, new instabilities were encountered for this new quantity, Δ, which shoots up and diverges rapidly. Therefore, an alternative is proposed. We consider the system (40) with the new term $T(t)$, given by (41). This is obtained by neglecting the term $\ddot{\Delta}$ in (39) (WKB approximation). The pressure and photon leakage terms are also neglected since they play no role at the times when this approximation is used. This system is integrated as long as condition $\left|\frac{k^2c^2}{4a^2}\delta_\gamma\right| \gg \left|\frac{T(t+\Delta t)-T(t))}{\Delta t}\right|$ is verified. When the condition is no longer fulfilled, the approximation is not valid anymore, and the complete equations (38) and (39) are integrated instead. In this way, the divergences present in the integration have been avoided and solutions will remain consistent.

$$\begin{cases} \dot{\Delta}(t) = \frac{\frac{k^2c^2}{4a^2}\delta_\gamma - \frac{T(t+\Delta t)-T(t)}{\Delta t}}{2\frac{\dot{a}}{a} + \sigma_T n_e c\left(\frac{\rho_\gamma}{\rho_{bar}} + \frac{3}{4}\right)} \\ \ddot{\delta}_\gamma + 2\frac{\dot{a}}{a}\dot{\delta}_\gamma = 2\left(\frac{\dot{a}}{a}\right)^2\left(\frac{\rho_{bar}}{\rho_t}\delta_{bar} + 2\frac{\rho_\gamma}{\rho_t}\delta_\gamma\right) + \sigma_T n_e c\dot{\Delta} - \frac{k^2}{3a^2}c^2\delta_\gamma \end{cases} \quad (40)$$

$$T(t) \equiv \frac{k^2c^2\delta_\gamma}{4a^2\left[2\frac{\dot{a}}{a} + \sigma_T n_e c\left(\frac{\rho_\gamma}{\rho_{bar}} + \frac{3}{4}\right)\right]} \quad (41)$$

In addition, as anticipated in section 2, numerical integration of expressions (38) and (39) is computationally expensive, because it requires performing a new integral, (23) and (27), at each time integration step. This is why a simplified alternative has been proposed as follows. At any given time t, it is considered that the distribution of λ_0 is an exponential characterized by $\bar{\lambda}$ (an assumption that holds true until shortly before the decoupling), and approximated by (42). In turn, we also first considered (29) and (30) valid at all times. To obtain $\bar{\lambda}$, we use the expression valid in the static case (first branch in (42)), as long as its time derivative grows more slowly than the horizon ($\dot{r}_{hor} = c/a(t)$). Otherwise, we assume that $\bar{\lambda}$ grows like the horizon (second branch in (42)).

$$\bar{\lambda}(t) = \begin{cases} \frac{1}{\sigma_T n_e(a) a} & t \le t_0 \\ \int_{t_0}^{t} \frac{c}{a(t)}dt & t > t_0 \end{cases} \quad (42)$$

$$\left[\frac{c}{a(t)}\right]_{t=t_0} = \left[\frac{d}{dt}\left(\frac{1}{\sigma_T n_e(a) a}\right)\right]_{t=t_0} \tag{43}$$

This methodology yields correct results until the moment of decoupling. From then on, the fluctuations δ_γ grow continuously, which is an incorrect behavior, as they should dampen over time. To avoid this result without having to perform integrals (23) and (27) at each integration step, the Montecarlo procedure has been followed, considering at each step a single value of λ_0, determined stochastically by (44).

$$\lambda_0 = \bar{\lambda}(t_0)(-ln(w)) + I(t) \qquad w \equiv \text{random}(0,1) \tag{44}$$

$$I(t) = \begin{cases} 0 & t \leq t_0 \\ \int_{t_0}^{t} \frac{c}{a(t')} dt' & t > t_0 \end{cases} \tag{45}$$

Functions $H(y)$ and $G(y)$ were obtained through interpolation fitting, whose representation can be seen in the appendix of this work (13), (**??**). So we will integrate the differential system (38) and (39) using the Euler method along with Friedmann equation (14), using the Runge-Kutta 4 method, and applying the methodologies described above. Lastly, we also want to note that, for some short time intervals, it was necessary to implement a smaller integration step size, also to overcome minor specific numerical instabilities. It was also necessary to set a lower limit of $5 \cdot 10^{-4}$ for the ionization fraction value, χ_e, as values below this caused instabilities that led the numerical solution to diverge.

5 Numerical results

To illustrate the relevance of each of the different terms in the evolution equations, we will first integrate the equations neglecting the leakage terms and using $H(k\bar{\lambda}) = 1/3$ (isotropic case), and compare this with the results obtained in [5]. Next, we will implement the correct function $H(k\bar{\lambda})$ (valid as long as λ_0 follows an exponential distribution) to observe the differences. These two integrations serve as an exercise to verify, afterwards, the effect of adding the leakage terms. In this way, the complete equations (including the leakage terms) will also be integrated using the $H(k\bar{\lambda})$ approximation, and finally, the results from applying the Montecarlo procedure, which is much more precise and where values of $\langle G(k\lambda_0)\rangle$ and $\langle V(k\lambda_0)\rangle$ are used, will be presented.

This procedure will be carried out separately, considering first a purely baryonic universe ($\Omega_{0,bar} = 0.04$) and later a universe with dark matter ($\Omega_{0,bar} = 0.04$, $\Omega_{0,DM} = 0.26$). This methodology has two important advantages. First, we ensure that the integration is correct and we can identify more easily and correct computational errors or instabilities. Secondly, this methodology will allow us to evaluate separately the influence of the different effects (already described) that take place in the evolution of the density fluctuations: photon diffusion, anisotropic angular distribution of photons or presence of dark matter, for example.

5.1 Purely baryonic universe

In first place, in a universe consisting only of baryons and photons, $\rho_{DM} = \Omega_{0,DM} = 0$, neglecting the terms related to photon leakage and considering an insotropic angular distribution of photons, equations (31), (32) and (14) simplify to (46) (47) and (48).

$$\ddot{\delta}_{k,\gamma} + 2\frac{\dot{a}}{a}\dot{\delta}_{k,\gamma} = \frac{16}{3}\pi G\left(\rho_{bar}\delta_{k,bar} + 2\rho_\gamma\delta_{k,\gamma}\right) + \frac{7}{12}\sigma_T n_e c\dot{\Delta} - \frac{1}{3}\frac{k^2}{a^2}c^2\delta_{k,\gamma} \tag{46}$$

$$\ddot{\Delta} + 2\frac{\dot{a}}{a}\dot{\Delta} = -\sigma_T n_e c\left(\frac{\rho_\gamma}{\rho_{bar}} + \frac{3}{4}\right)\dot{\Delta} + \frac{k^2}{4a^2}c^2\delta_{k,\gamma} \tag{47}$$

$$H = H_0\sqrt{\Omega_{0,bar}a^{-3} + \Omega_{0,rad}a^{-4} + \Omega_{0,k}a^{-2}} \tag{48}$$

Results from integration at different scales are shown in Figure 2, in comparison with those obtained in [5]. In particular, mass scale $M = 4.74 \cdot 10^{14}\ M_\odot$ has been plotted, as it is the

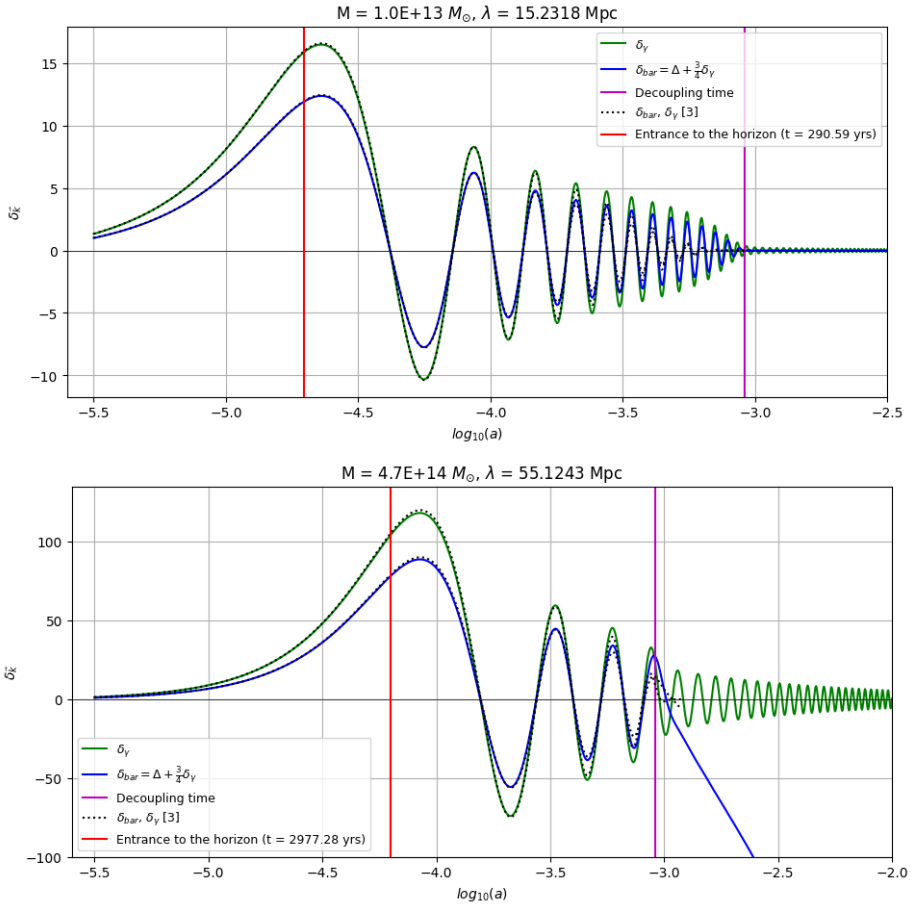

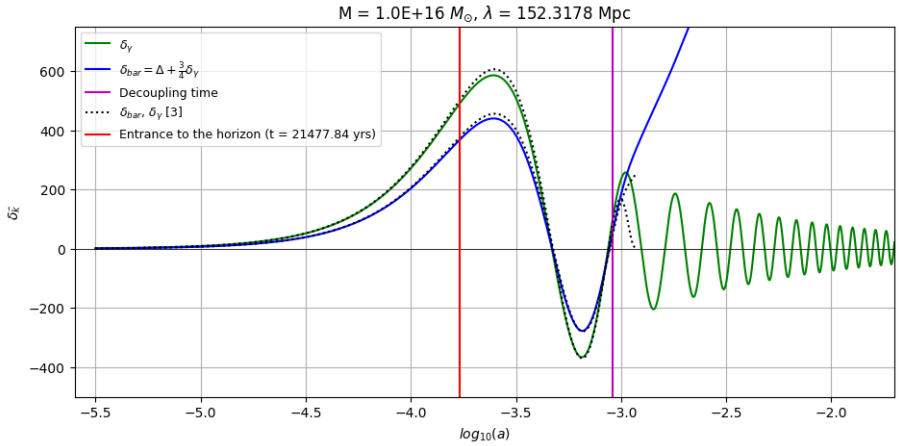

Figure 2: Density fluctuations evolution of photons (green) and baryons (blue), obtained from equations (46), (47) for different scales, along with solutions in [5].

value of Silk mass considering a pure baryonic universe (19). It can be seen how the solutions are similar, although, especially at smaller scales, fluctuation oscillations obtained in [5] are rather more damped. This difference is expected to be corrected when adding photon leakage terms, which, as explained, cause an additional damping of the oscillations (keep in mind that there will always be some damping of the oscillations due to the expansion of the universe).

In Figure 2, it can also be seen that this treatment is not suitable to describe the evolution of fluctuations beyond decoupling. From this time, amplitude of photonic fluctuations is expected to decrease much faster. Since photons stop interacting with matter, their mean free path, $\bar{\lambda}$, increases significantly, so they start free streaming behavior and their oscillations should dampen considerably.

5.1.1 The effect of photon angular distribution anisotropies: Implementation of $H(k\bar{\lambda})$

Introducing, now, the function $H(k\bar{\lambda})$ instead of the factor 1/3, in the photon-photon pressure term, that account for the anisotropies present in the angular distribution of photons, we integrate equations (49) and (50).

$$\ddot{\delta}_{k,\gamma} + 2\frac{\dot{a}}{a}\dot{\delta}_{k,\gamma} = \frac{16}{3}\pi G\left(\rho_{bar}\delta_{k,bar} + 2\rho_\gamma\delta_{k,\gamma}\right) + \frac{7}{12}\sigma_T n_e c\dot{\Delta} - \frac{k^2}{a^2}c^2 H(k\bar{\lambda})\delta_{k,\gamma} \tag{49}$$

$$\ddot{\Delta} + 2\frac{\dot{a}}{a}\dot{\Delta} = -\sigma_T n_e c\left(\frac{\rho_\gamma}{\rho_{bar}} + \frac{3}{4}\right)\dot{\Delta} + \frac{3k^2}{4a^2}c^2 H(k\bar{\lambda})\delta_{k,\gamma} \tag{50}$$

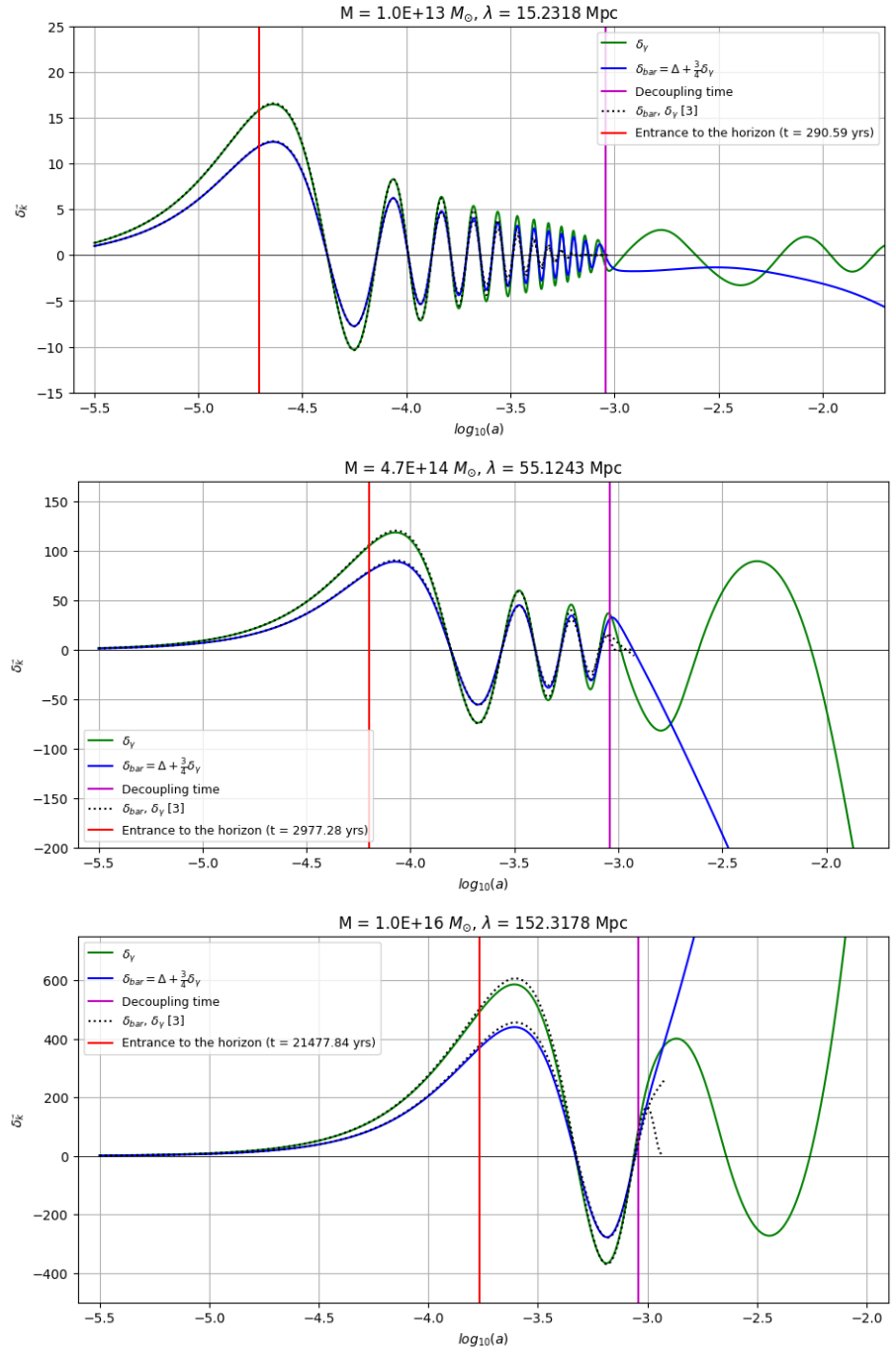

Figure 3: Density fluctuations evolution of photons (green) and baryons (blue), obtained from equations (49), (50) for different scales, along with solutions in [5].

When comparing solutions represented in Figure 2 with those in Figure 3, we can see that the effect of the anisotropy is to decrease the damping of oscillations, whose amplitudes are now slightly higher, as they approach the decoupling time, t_{dec} (see Table 1).

5.1.2 The effect of photon diffusion: Implementation of photon leakage terms

Equations (51) and (52) contain all the terms present in the evolution of density fluctuations. Before integrating the exact relations, the results obtained using approximations (29) and (30) at every time are shown in Figure 4.

$$\ddot{\delta}_{k,\gamma} + 2\frac{\dot{a}}{a}\dot{\delta}_{k,\gamma} = \frac{16}{3}\pi G\left(\rho_{bar}\delta_{k,bar} + 2\rho_{\gamma}\delta_{k,\gamma}\right) + \frac{7}{12}\sigma_T n_e c\left(\dot{\delta}_{k,bar} - \frac{3}{4}\dot{\delta}_{k,\gamma}\right) - \frac{k^2}{a^2}c^2 H(k\bar{\lambda})\delta_{k,\gamma} - \frac{\dot{a}}{a}\frac{kc}{a}[k\bar{\lambda}H(k\bar{\lambda})] - \frac{kc}{a}[k\bar{\lambda}H(k\bar{\lambda})]\dot{\delta}_{k,\gamma} - \frac{k^2 c}{a}H(k\bar{\lambda})\dot{\bar{\lambda}}\delta_{k,\gamma} \quad (51)$$

$$\ddot{\Delta} + 2\frac{\dot{a}}{a}\dot{\Delta} = -\sigma_T n_e c\left(\frac{\rho_{\gamma}}{\rho_{bar}} + \frac{3}{4}\right)\dot{\Delta} + \frac{3k^2}{4a^2}c^2\delta_{k,\gamma}H(k\bar{\lambda}) + \frac{3}{4}\frac{\dot{a}}{a}\frac{kc}{a}[k\bar{\lambda}H(k\bar{\lambda})] + \frac{3}{4}\frac{kc}{a}[k\bar{\lambda}H(k\bar{\lambda})]\dot{\delta}_{k,\gamma} + \frac{3}{4}\frac{k^2 c}{a}H(k\bar{\lambda})\dot{\bar{\lambda}}\delta_{k,\gamma} \quad (52)$$

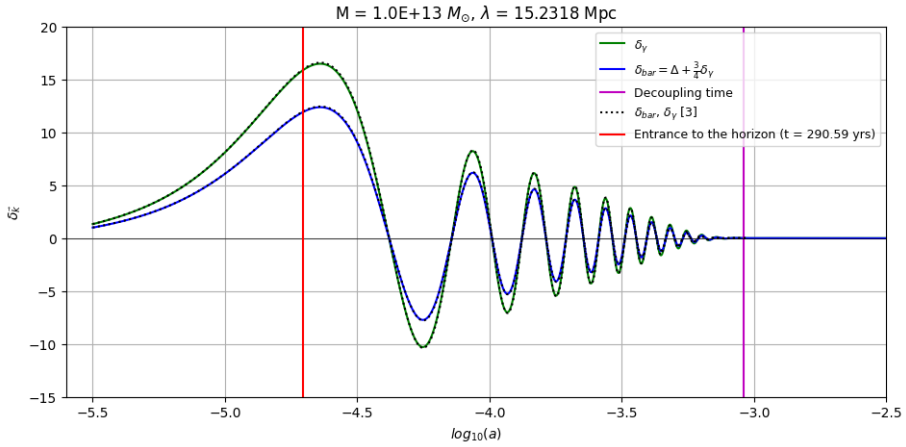

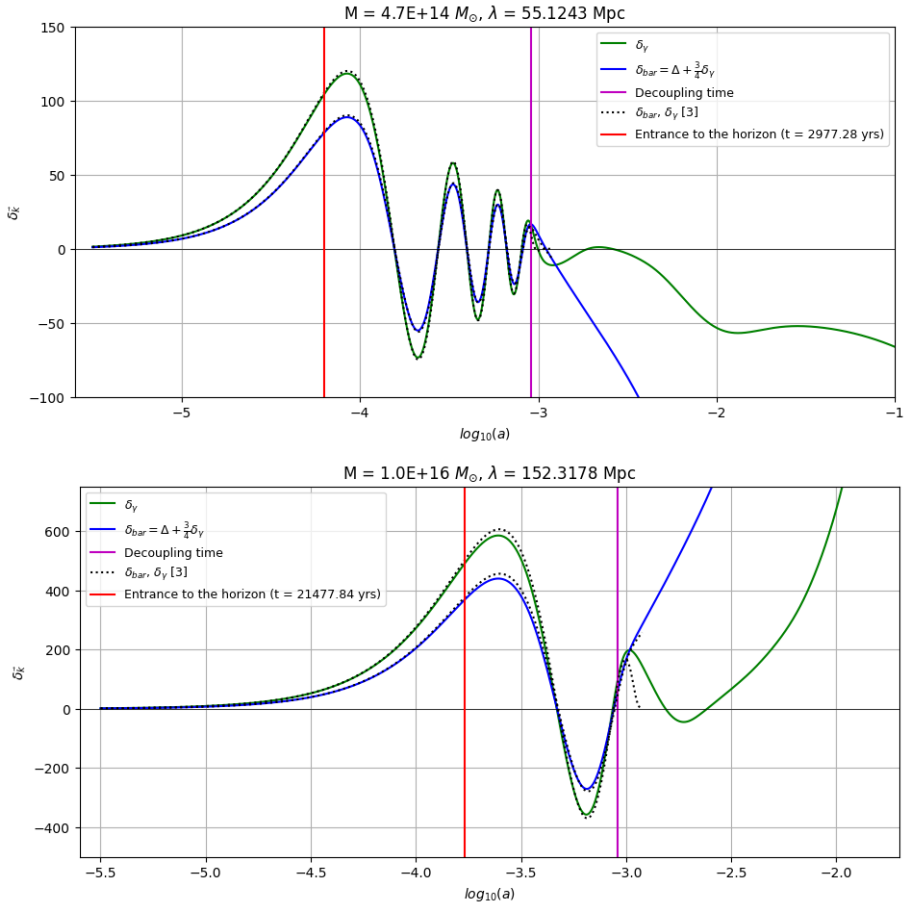

Figure 4: Density fluctuations evolution of photons (green) and baryons (blue), obtained from equations (51), (52) for different scales, along with solutions in [5].

It can be seen that, now that photon leakage terms are included, solutions are very similar with that obtained in [5], at $t < t_{dec}$. It is thus confirmed that the photon diffusion effect produces additional damping.

At this point, it is convenient to make an explicit comparison of these results with those obtained in [5]. Figure 5 and Figure 6 show the amplitudes and times corresponding to each of the baryonic oscillation peaks. It can be seen that the numerical results are very close between both formalisms.

It is important to note that the approximated formalism used in [5] remains valid at times $t_{hor} < t < t_{dec}$, so it is expected that the solutions in both cases coincide. However, as mentioned before, relativistic corrections must be applied for $t \lesssim t_{hor}$, while the exact equations used in this work are necessary for $t > t_{dec}$, as well as a more precise integration

method, which is studied in next subsection.

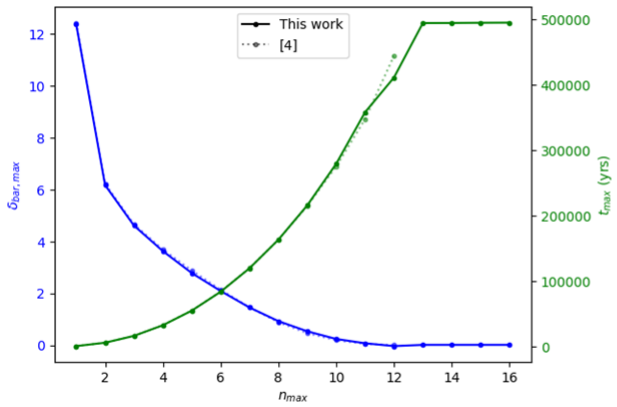

$\delta_{bar,max}$		t_{max} (yrs)	
This work	TFG [5]	This work	TFG [5]
12.379	12.436	$3.95 \cdot 10^2$	$3.97 \cdot 10^2$
6.170	6.225	$5.57 \cdot 10^4$	$5.58 \cdot 10^4$
4.609	4.660	$1.61 \cdot 10^4$	$1.61 \cdot 10^4$
3.626	3.687	$3.23 \cdot 10^4$	$3.24 \cdot 10^4$
2.780	2.882	$5.46 \cdot 10^4$	$5.48 \cdot 10^4$
2.088	2.139	$8.35 \cdot 10^4$	$8.38 \cdot 10^4$
1.451	1.458	$1.19 \cdot 10^5$	$1.20 \cdot 10^5$
0.926	0.884	$1.63 \cdot 10^5$	$1.63 \cdot 10^5$
0.534	0.460	$2.16 \cdot 10^5$	$2.15 \cdot 10^5$
0.238	0.190	$2.79 \cdot 10^5$	$2.75 \cdot 10^5$
0.0731	0.048	$3.58 \cdot 10^5$	$3.47 \cdot 10^5$

Figure 5: Amplitudes (blue) and times (green) of each baryonic oscillation peak for $M = 10^{13}\ M_\odot$, obtained in [5] (dashed) and in this work (solid).

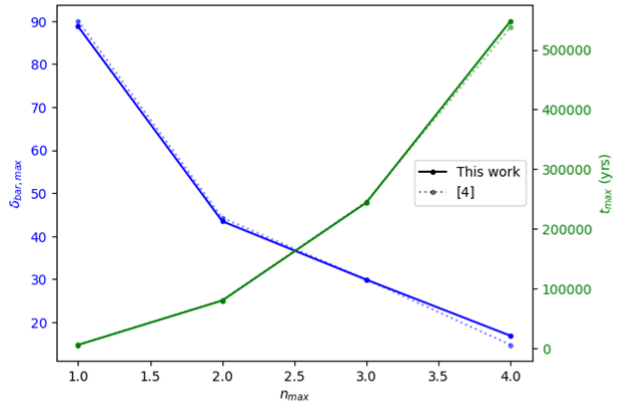

$\delta_{bar,max}$		t_{max} (yrs)	
This work	TFG [5]	This work	TFG [5]
88.75	90.07	$5.34 \cdot 10^3$	$5.40 \cdot 10^3$
43.47	44.24	$7.97 \cdot 10^4$	$8.02 \cdot 10^4$
29.87	29.93	$3.44 \cdot 10^5$	$2.44 \cdot 10^5$
16.84	14.74	$5.49 \cdot 10^5$	$5.38 \cdot 10^5$

Figure 6: Amplitudes (blue) and times (green) of each baryonic oscillation peak for $M = 4.74 \cdot 10^{14}\ M_\odot$, obtained in [5] (dashed) and in this work (solid).

For a better understanding of these results, compared to those obtained previously in [5], ratios between the amplitudes of baryonic oscillations at the horizon crossing time and at the moment of the first oscillation peak are shown in Table 1.

M ($M_\odot$)	$\delta_{bar}(t_{hor})/\delta_{bar}(t_{peak\ 1})$		$t_{hor}/t_{peak\ 1}$	
	This work	TFG [5]	This work	TFG [5]
10^{13}	1.539	1.539	$12.38 \cdot 10^{-2}$	$12.34 \cdot 10^{-2}$
10^{14}	1.458	1.453	$10.08 \cdot 10^{-2}$	$10.02 \cdot 10^{-2}$
$4.74 \cdot 10^{14}$	1.419	1.412	$9.12 \cdot 10^{-2}$	$9.04 \cdot 10^{-2}$
10^{15}	1.404	1.396	$8.72 \cdot 10^{-2}$	$8.62 \cdot 10^{-2}$
10^{16}	1.360	1.352	$7.37 \cdot 10^{-2}$	$7.22 \cdot 10^{-2}$

Table 1: Ratios between baryonic fluctuations at the horizon crossing time and at first oscillation peak, for different scales, in a purely baryonic universe.

Numerical values corresponding to TFG [5] have been recalculated, using the same equations in [5], but with a better approximation for the horizon radius, $r_{hor}(t)$.

In addition, in Table 2, we have collected the peak values of baryonic fluctuations, for each considered case. It can be observed that approximation $H(k\bar{\lambda}) = 1/3$ describes well the fluctuations at early times. However, as oscillations approach the decoupling time, its amplitudes decrease too much, since the anisotropies in the angular distribution of photons are being neglected. Nevertheless, this correction is very small in comparison with the effect produced by the photon leakage terms. It is evident that this effect significantly damps the fluctuations, resulting in much smaller peaks in this case, and even eliminating by Silk dampling perturbations of certain scales ($M = 10^{13}\ M_\odot$) which, if this effect were not taken into account, would have survived until the moment of decoupling.

M ($M_\odot$)	Case	$\delta_{bar_{max}}$								
10^{13}	$H = 1/3$	12.37	6.22	4.79	4.04	3.57	3.22	2.93	2.66	2.36
	$H(k\bar{\lambda})$	12.37	6.22	4.79	4.04	3.57	3.23	2.94	2.68	2.40
	Photon leakage	12.37	6.17	4.61	3.63	2.82	2.14	1.52	0.97	0.55
$4.74 \cdot 10^{14}$	$H = 1/3$	88.72	44.78	34.25	28.23					
	$H(k\bar{\lambda})$	88.72	44.79	34.31	32.76					
	Photon leakage	88.75	43.47	29.87	16.84					
10^{16}	$H = 1/3$	439.56								
	$H(k\bar{\lambda})$	439.58								
	Photon leakage	439.15								

Table 2: Peaks of baryonic fluctuations, δ_{bar}, in each of the considered cases, for different scales.

All this numerical comparisons have been done using solutions obtained in this subsection, with approximations (29) and (30), since they are completely valid within the time integration intervals we are analyzing, and they do not generate the small stochastic errors that Montecarlo method may present.

5.1.3 Precise solution: Montecarlo procedure

As we have just seen, approximations (29) and (30) accurately describe the evolution of fluctuations until $t \lesssim t_{dec}$. However, beyond this time, this approximation is no longer valid for integrating the equations, since the probability distribution of λ_0 is not an exponential anymore. Therefore, we use the Montecarlo method, with λ_0 given stochastically at each integration step as indicated in (44). In this subsection, we show the results obtained from solving the exact equations, in a purely barionic universe, applying this Montecarlo procedure.

$$\ddot{\delta}_{k,\gamma} + 2\frac{\dot{a}}{a}\dot{\delta}_{k,\gamma} = \frac{16}{3}\pi G\left(\rho_{bar}\delta_{k,bar} + 2\rho_\gamma\delta_{k,\gamma}\right) + \frac{7}{12}\sigma_T n_e c\left(\dot{\delta}_{k,bar} - \frac{3}{4}\dot{\delta}_{k,\gamma}\right) - \frac{k^2}{a^2}c^2\langle G(k\lambda_0)\rangle\delta_{k,\gamma} - \frac{\dot{a}}{a}\frac{kc}{a}\langle V(k\lambda_0)\rangle - \frac{kc}{a}\langle V(k\lambda_0)\rangle\dot{\delta}_{k,\gamma} - \frac{k^2c}{a}\langle G(k\lambda_0)\rangle\dot{\bar{\lambda}}\delta_{k,\gamma} \quad (53)$$

$$\ddot{\Delta} + 2\frac{\dot{a}}{a}\dot{\Delta} = -\sigma_T n_e c\left(\frac{\rho_\gamma}{\rho_{bar}} + \frac{3}{4}\right)\dot{\Delta} + \frac{3k^2}{4a^2}c^2\delta_{k,\gamma}\langle G(k\lambda_0)\rangle + \frac{3}{4}\frac{\dot{a}}{a}\frac{kc}{a}\langle V(k\lambda_0)\rangle + \frac{3}{4}\frac{kc}{a}\langle V(k\lambda_0)\rangle\dot{\delta}_{k,\gamma} + \frac{3}{4}\frac{k^2c}{a}\langle G(k\lambda_0)\rangle\dot{\bar{\lambda}}\delta_{k,\gamma} \quad (54)$$

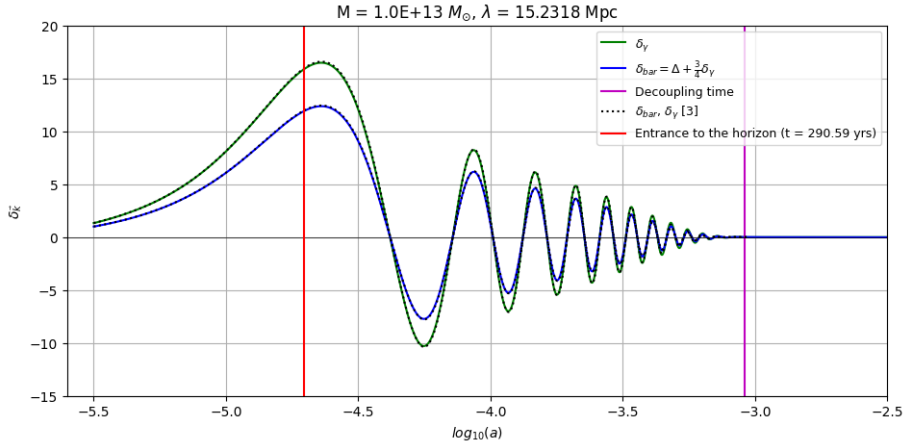

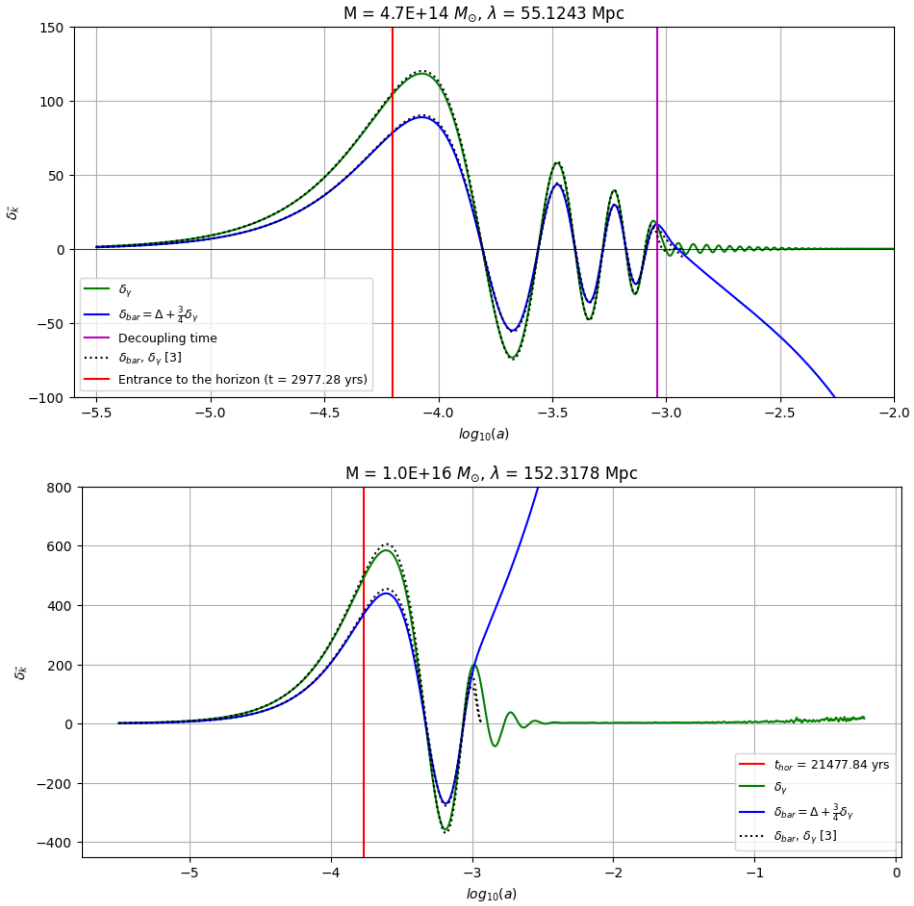

Figure 7: Density fluctuations evolution of photons (green) and baryons (blue), obtained from equations (53), (54) with Montecarlo procedure for different scales, along with solutions in [5].

With this last methodology, we have obtained numerical solutions of (53) and (54) that indeed describe density fluctuations, both at $t \lesssim t_{dec}$ and for t after the radiation-matter decoupling. Scale $M = 10^{13}\ M_\odot$ experiences Silk damping, resulting in a complete suppression of fluctuations. However, scales $M = 4.74 \cdot 10^{14}\ M_\odot$ and $M = 10^{16}\ M_\odot$ show how, post-decoupling, photon fluctuations persist but are heavily damped due to the free streaming effect.

Drag time and fluctuation scales

The time when baryons are released from the drag of photons is called **drag time**, t_{drag}, or drag epoch z_d. It can be interpreted as the moment when the gravitational force surpasses the radiation pressure in the radiation-matter interaction. It's important to distinguish this

time from the decoupling time, t_{dec}, which occurs slightly earlier. In this subsection, we estimate the drag time values for different fluctuation scales, as a practical application of the solutions obtained in 5.1.2, in the case of a purely baryonic universe.

$M\ (M_\odot)$	10^{13}	10^{14}	$4.74 \cdot 10^{14}$	10^{15}	10^{16}	10^{17}
$a(t_{drag})$	$1.222 \cdot 10^{-3}$	$1.248 \cdot 10^{-3}$	$1.231 \cdot 10^{-3}$	$1.230 \cdot 10^{-3}$	$1.206 \cdot 10^{-3}$	$1.209 \cdot 10^{-3}$

Table 3: Scale factor at drag time for different scales in a purely baryonic universe.

In practice, we have defined the drag time as the moment when the right-hand side of baryonic fluctuations equation (32) has the same sign as the density of baryonic fluctuations, δ_{bar}. In Table 3, we show the drag times obtained, using solutions from 5.1.2, for different scales. Although this solutions are only valid at $t < t_{dec}$, given the proximity of the decoupling time with the drag time, it has also been considered valid for this analysis. It can be seen that, for all considered scales, the obtained drag time is always higher than the decoupling time, which we have considered as $a_{dec} \sim 9.9 \cdot 10^{-4}$ ($3.8 \cdot 10^5$ years). Also, in Figure 8 we have plotted the evolution of the gravitational term and the radiation pressure term from (32) for $M = 10^{14}\ M_\odot$.

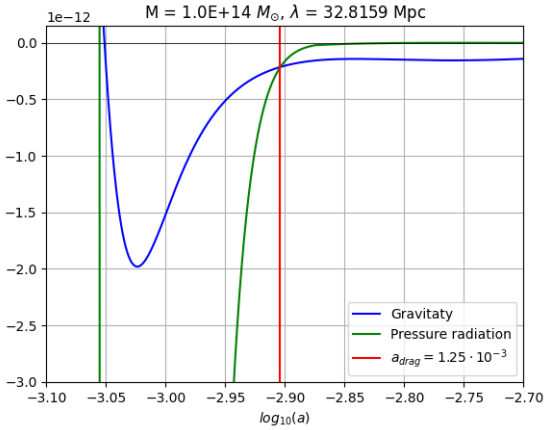

Figure 8: Evolution of gravitational interaction and photons pressure for $M = 10^{14}\ M_\odot$. The scale factor a_{drag} corresponds with the moment when gravity is higher, in absolute value, than radiation pressure.

5.2 Universe with dark matter

Considering now the presence of dark matter, $\rho_{DM} \neq 0$ and $\Omega_{0,DM} = 0.26$, we will first integrate the complete equations (55), (56) and (57) with (58) using the approximations $\langle G(K\lambda_0)\rangle = H(k\bar{\lambda})$ and $\langle V(k\lambda_0)\rangle = k\bar{\lambda}H(k\bar{\lambda})$ at every integration time. Finally, we will

show the solutions of the exact equations, using the Montecarlo procedure.

$$\ddot{\delta}_{k,\gamma} + 2\frac{\dot{a}}{a}\dot{\delta}_{k,\gamma} = \frac{16}{3}\pi G\left(\rho_{bar}\delta_{k,bar} + 2\rho_\gamma\delta_{k,\gamma} + \rho_{DM}\delta_{k,DM}\right) + \frac{7}{12}\sigma_T n_e c\left(\dot{\delta}_{k,bar} - \frac{3}{4}\dot{\delta}_{k,\gamma}\right) - \frac{k^2}{a^2}c^2\langle G(k\lambda_0)\rangle\delta_{k,\gamma} - \frac{\dot{a}}{a}\frac{kc}{a}\langle V(k\lambda_0)\rangle - \frac{kc}{a}\langle V(k\lambda_0)\rangle\dot{\delta}_{k,\gamma} - \frac{k^2c}{a}\langle G(k\lambda_0)\rangle\dot{\bar{\lambda}}\delta_{k,\gamma} \quad (55)$$

$$\ddot{\Delta} + 2\frac{\dot{a}}{a}\dot{\Delta} = -\sigma_T n_e c\left(\frac{\rho_\gamma}{\rho_{bar}} + \frac{3}{4}\right)\dot{\Delta} + \frac{3k^2}{4a^2}c^2\delta_{k,\gamma}\langle G(k\lambda_0)\rangle + \frac{3}{4}\frac{\dot{a}}{a}\frac{kc}{a}\langle V(k\lambda_0)\rangle + \frac{3}{4}\frac{kc}{a}\langle V(k\lambda_0)\rangle\dot{\delta}_{k,\gamma} + \frac{3}{4}\frac{k^2c}{a}\langle G(k\lambda_0)\rangle\dot{\bar{\lambda}}\delta_{k,\gamma} \quad (56)$$

$$\ddot{\delta}_{DM} + 2\frac{\dot{a}}{a}\dot{\delta}_{DM} = 4\pi G\left(\rho_{bar}\delta_{bar} + 2\rho_\gamma\delta_\gamma + \rho_{DM}\delta_{k,DM}\right) \quad (57)$$

$$\frac{\dot{a}}{a} = H_0\sqrt{\left(\Omega_{0,bar} + \Omega_{0,DM}\right)a^{-3} + \Omega_{0,\gamma}a^{-4} + \Omega_{0,k}a^{-2}} \quad (58)$$

5.2.1 Approximate solution

In Figure 9, we can see again that approximations (29) and (30) are not valid after the decoupling, as the behavior of photons after that time is incorrect. As we have mentioned, after decoupling, photons do not interact with matter, instead, they experience free streaming, propagating freely through the universe. In this way, their fluctuations should not grow as they do in 9. However, baryonic fluctuations behavior seems to be correct. Scale $M = 4.74 \cdot 10^{14}\ M_\odot$ has been plotted in logarithmic scale, to better observe how baryonic fluctuations grow rapidly, once they have decoupled from photons, to match the growth rate of dark matter fluctuations.

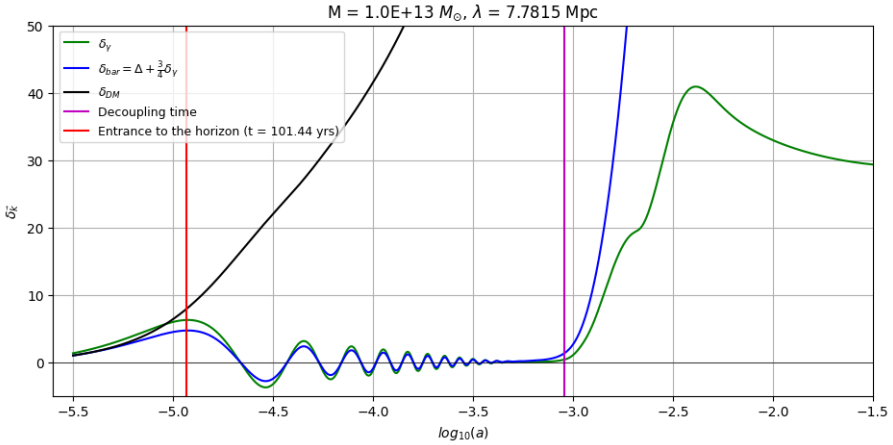

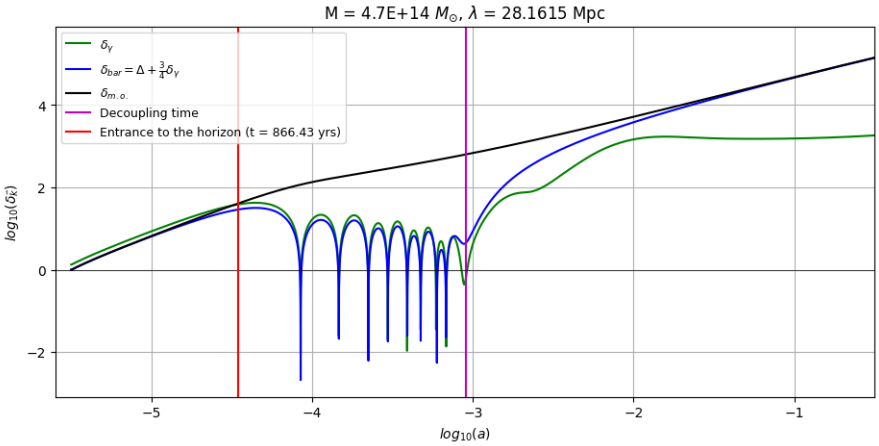

Figure 9: Density fluctuations evolution of photons (green), baryons (blue) and dark matter (black), obtained from equations (55), (56) and (57) with approximations (29) and (30) for different scales.

M ($M_\odot$)	$\delta_{bar}(t_{hor})/\delta_{bar}(t_{peak\ 1})$		$t_{hor}/t_{peak\ 1}$	
	This work	TFG [5]	This work	TFG [5]
10^{13}	1.678	1.550	$16.63 \cdot 10^{-2}$	$20.30 \cdot 10^{-2}$
10^{14}	1.708	1.581	$11.73 \cdot 10^{-2}$	$13.78 \cdot 10^{-2}$
$4.74 \cdot 10^{14}$	1.787	1.530	$10.04 \cdot 10^{-2}$	$10.78 \cdot 10^{-2}$
10^{15}	1.869	1.497	$9.41 \cdot 10^{-2}$	$9.48 \cdot 10^{-2}$

Table 4: Ratios between baryonic fluctuations at the horizon crossing time and at first oscillation peak, for different scales, in a universe with dark matter.

5.2.2 Precise solution: Montecarlo procedure

Applying this methodology, λ_0 is, at each time step, stochastically determined, so it is, as already emphasized, a suitable numerical method to solve the exact equations. As it can be seen in Figure 10 and Figure 11, solutions obtained with this procedure align well with the expected behavior of density fluctuations δ_γ, δ_{bar} and δ_{DM}. Similarly to the previous case, some scales have been represented on a logarithmic scale to facilitate the visualization of the results. The "oscillations" observed at the end of scales $M = 4.74 \cdot 10^{14} M_\odot$ and $M = 1 \cdot 10^{16}\ M_\odot$ are due to stochastic noise.

Dark matter does not interact electromagnetically and does not emit or absorb light. Due to this non-collisional nature, dark matter perturbations continue growing without a practical limit in scale, unlike baryons, which, as we have seen, are influenced by radiation pressure and other electromagnetic forces that limit their collapse to smaller scales. In this way, until decoupling time, photons and baryons remain oscillating together. Once baryonic matter

is decoupled from radiation, it evolves under the gravitational influence of dark matter, so baryonic fluctuations grow until they match the growth rate of dark matter perturbations. At this time, photons do not interact electromagnetically, so they diffuse away from baryonic fluctuations and their oscillations dampen very quickly.

We have included the plotting of $M = 10^{15}\ M_{\odot}$, since we would like to compare it with the obtained in [6] (Figure 11). Even though the units of the perturbations δ are arbitrary, it can be seen, qualitatively, that the solutions of the exact equations (55), (56) and (57), obtained through this methodology, are very similar with that illustrated in Figure 11.

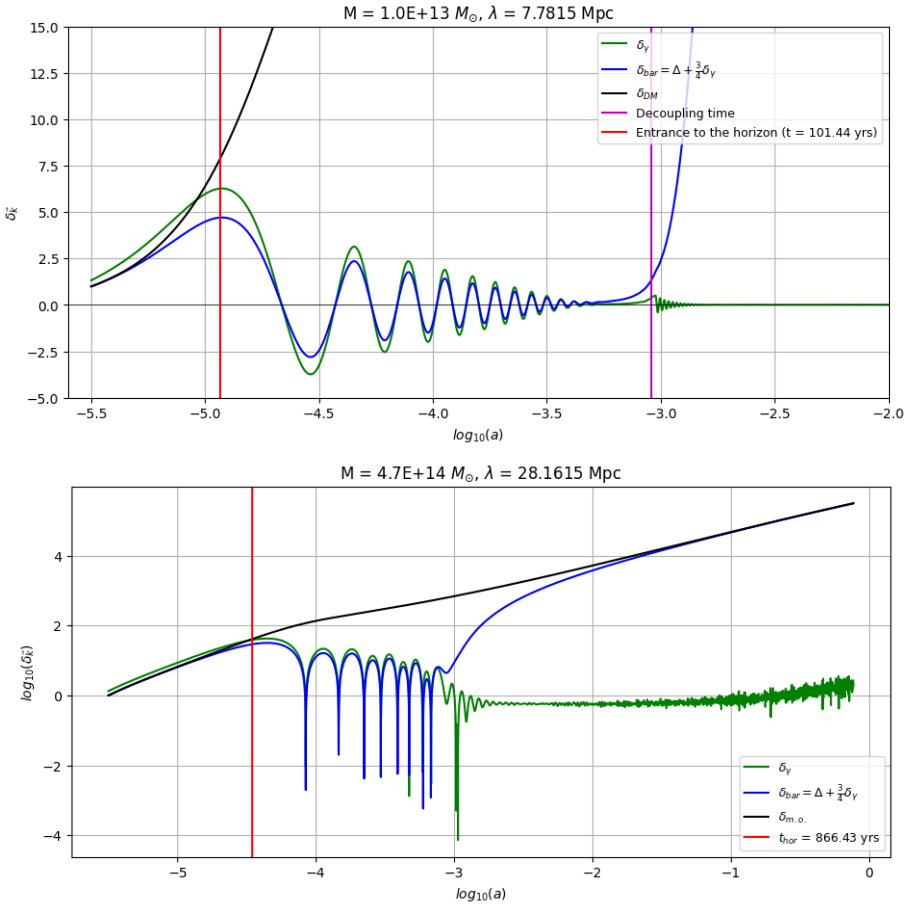

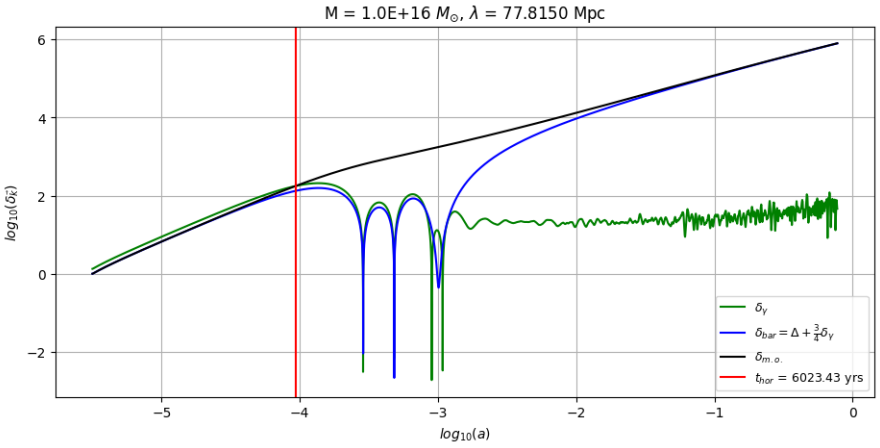

Figure 10: Density fluctuations evolution of photons (green), baryons (blue) and dark matter (black), obtained from equations (55), (56) and (57) with Montecarlo procedure for different scales.

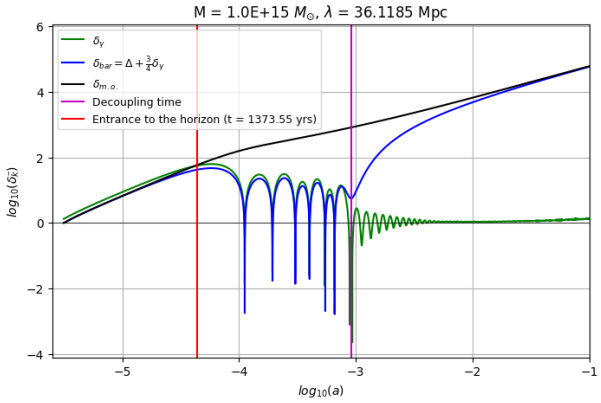

Figure 11: Density fluctuations evolution of photons (green), baryons (blue) and dark matter (black), obtained from equations (55), (56) and (57) with Montecarlo procedure for $M = 10^{15}\ M_\odot$ in logarithmic scale (left). Density fluctuations, in the same case, illustrated in [6] (right).

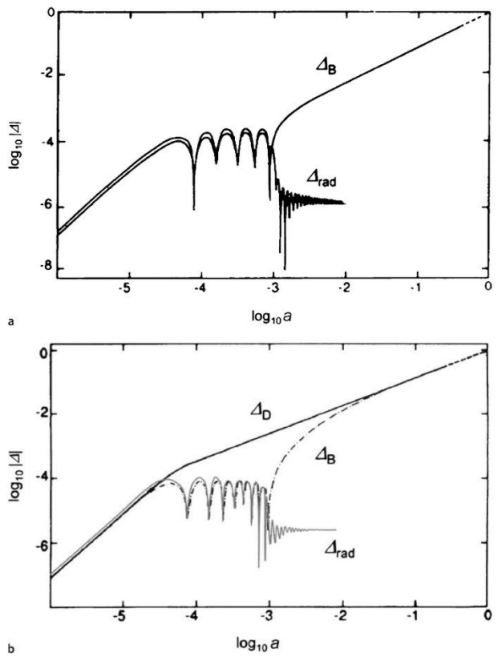

Fig. 13.3a,b. Illustrating the evolution of density perturbations in **a** baryonic matter Δ_B and radiation Δ_{rad} in the standard baryonic adiabatic model and **b** the baryonic matter Δ_B, the radiation Δ_{rad} and the dark matter Δ_D according to the cold dark matter scenario. In both cases, the mass of the perturbation is $M \sim 10^{15}\ M_\odot$ (Coles and Lucchin, 1995)

6 Relativistic corrections

Until now, a quasi-Newtonian (or non-relativistic) formalism has been used. This interpretation is only valid for times $t > t_{hor}$, as it predicts an artificial growth of density fluctuations for earlier times ($t \lesssim t_{hor}$). In this work, a first attempt is made to derive new equations to characterize the behavior of fluctuations at $t \lesssim t_{hor}$. At the limit $t \ll t_{hor}$, a logarithmic growth should occur, which is accurately reproduced by the equations presented here (Betancort-Rijo 2024). In this relativistic case, neutrino density fluctuations, δ_ν, must be taken into account. The equation for their evolution (61) is essentially a simplification of that for photons (31), since neutrinos are decoupled from matter at all times t. Thus, neutrinos mean free path is equal to the horizon radius, $r_{hor}(t)$, at all t, so, in this case, it is not necessary to average G and V functions over the neutrinos mean free path.

$$\ddot{\delta}_\gamma + 2\frac{\dot{a}}{a}\dot{\delta}_\gamma = \frac{16\pi G}{3}\left(\rho_{bar}\delta'_{bar} + 2\rho_\gamma\delta'_\gamma + 2\rho_\nu\delta'_\nu\right) + \frac{7}{12}\sigma_T n_e c\dot{\Delta} - \frac{k^2}{a^2}c^2\delta_\gamma H(k\bar{\lambda}) - \frac{\dot{a}}{a}\frac{kc}{a}\langle V(k\lambda_0)\rangle - \frac{kc}{a}\langle V(k\lambda_0)\rangle\dot{\delta}_\gamma - \frac{k^2c}{a}\langle G(k\lambda_0)\rangle\dot{\bar{\lambda}}\delta_\gamma \quad (59)$$

$$\ddot{\Delta} + 2\frac{\dot{a}}{a}\dot{\Delta} = -\frac{7}{12}\sigma_T n_e c\left(\frac{\rho_\gamma}{\rho_{bar}} + \frac{3}{4}\right)\dot{\Delta} + \frac{3}{4}\frac{k^2}{a^2}c^2\delta_\gamma H(k\bar{\lambda}) + + \frac{3}{4}\frac{kc}{a}\dot{\delta}_\gamma\langle V(k\lambda_0)\rangle + \frac{3}{4}\frac{k^2c}{a}\delta_\gamma\langle G(k\lambda_0)\rangle\dot{\bar{\lambda}} + \frac{3}{4}\frac{\dot{a}}{a}\frac{kc}{a}\langle V(k\lambda_0)\rangle\delta_\gamma \quad (60)$$

$$\ddot{\delta}_\nu + 2\frac{\dot{a}}{a}\dot{\delta}_\nu = \frac{16\pi G}{3}\left(\rho_{bar}\delta'_{bar} + 2\rho_\gamma\delta'_\gamma + 2\rho_\nu\delta'_\nu\right) - 2\frac{k^2c^2}{a^2}G(kr_{hor}(t))\delta_\nu - \frac{kc}{a}V(kr_{hor}(t))\dot{\delta}_\nu - \frac{\dot{a}}{a}V(kr_{hor}(t))\frac{kc}{a}\delta_\nu \quad (61)$$

Although (59), (60) and (61) are not the exact relations, we will see that they describe properly the evolution of perturbations at $t \ll t_{hor}$. Since the effect of these corrections is significantly only at $t < t_{hor}$, we can use approximations (29) and (30) to solve these relativistic equations. To avoid computational instabilities that arise when attempting to integrate equation (61), an approximate integrated expression (62) is used for describe the neutrino density perturbations.

$$\delta_\nu = \delta_\nu(t_{in})\frac{sen(kr_{hor}(t))}{kr_{hor}(t)}\frac{kr_{hor}(t_{in})}{kr_{hor}(t_{in})} + + \frac{16\pi Ga^2}{c^2k^2}\left(\rho_{bar}(t)\delta'_{bar} + 2\rho_\gamma\delta'_\gamma + 2\rho_\nu\delta'_\nu\right)\left(1 - \frac{sen(kr_{hor}(t) - r_{hor}(t_{in}))}{k(r_{hor}(t) - r_{hor}(t_{in}))}\right) \quad (62)$$

By integrating (59) and (60) using (62) and the new initial conditions $\delta_\nu(t_{in}) = \delta_\gamma(t_{in}) = 4/3$ and $\dot{\delta}_\gamma(t_{in}) = \dot{\delta}_{bar}(t_{in}) = \dot{\delta}_\nu(t_{in}) = 0$, we get the solutions represented in Figure 12. These

approximate equations that have been used assume corrections for $t < t_{hor}$, so we will not focus on observed behavior after t_hor. It can be seen that now, before the entry to the horizon, we no longer have that erroneous growth of the perturbations that we had been observing with the non-relativistic treatment.

In addition, solutions density perturbations of neutrinos have been obtained and represented in Figure 12. As we mentioned, neutrinos do not interact with baryons and photons, so, when these fluctuations enter the horizon, they start to oscillate because of their own pressure, independently of the rest of the constituents. Neutrino oscillations experience damping due to neutrino diffusion, similar to photon oscillations. Recall that equations for photons (59) and neutrinos (61) are practically the same, except for the coupling term, and the dependencies of the leakage terms.

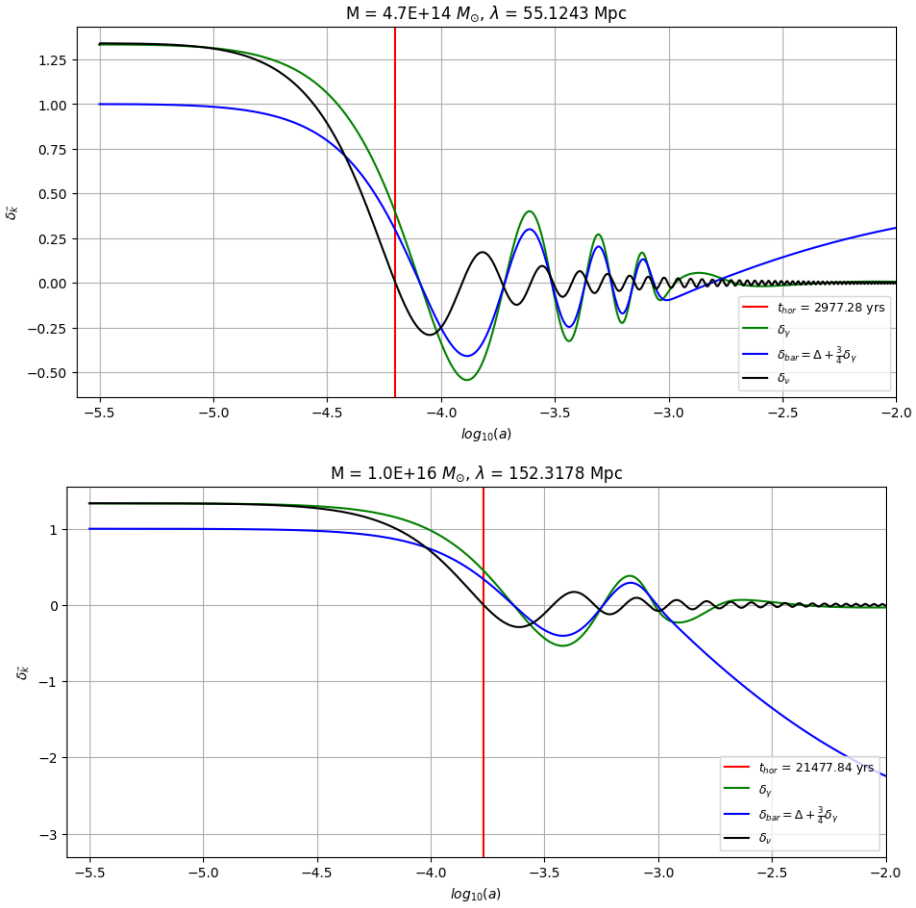

Figure 12: Density fluctuations evolution of photons (green), baryons (blue) and neutrinos (black), obtained from relativistic equations (59), (60) and (62) with approximations (29) and (30) for different scales, in a purely baryonic universe.

7 Conclusions

This work has involved the numerical resolution of exact equations of evolution of density fluctuations of photons, δ_γ, baryons, δ_{bar} and dark matter, δ_{DM}. Given by (31), (32) and (33), we have seen that this equations describe adequately the behavior and evolution of this perturbations. Throughout the resolution of the equations and the analysis of its solutions, we have studied the effect of the different terms that constitute them, as well as the interactions between the considered components: radiation, baryonic matter and dark matter. In addition, we have used several numerical methods and approximations, both analytical and numerical, to solve the expressions in the most precise and efficient manner (aiming to save computational costs).

In first place, we treated the case of a purely baryonic universe. In subsection 5.1.1, we have seen that the radiation pressure term must be modulated by a function of λ_0, the photon mean free path, to take into account the anisotropies present in photon angular distribution. Solutions indicate that, with this small correction, oscillations have higher amplitudes (Table 1), as photons exhibit slightly more diffuse movements due to this anisotropy.

Then, we have included the terms corresponding to photon leakage, and it has been seen that this diffusion effect of radiation is crucial in the damping of the perturbations. With this terms, we already have the complete equations of evolution of density fluctuations. We have used two different procedures to solve the exact equations. First, approximations (29) and (30), formulated to be valid at $t \lesssim t_{dec}$, were found to be consistent with that obtained in previous work [5] (Figure 5 and Figure 6). Later, by solving the equations with Montecarlo procedure, we obtained solutions that properly describe the behavior of fluctuations beyond t_{dec}, when the effect of free streaming shows up.

Later, we considered the case of a universe with dark matter. As in the previous case, equations were first solved approximately and it was verified that, also in this case, this method is valid for $t \lesssim t_{dec}$. At times $t > t_{dec}$, Montecarlo procedure was necessary to solve the equations correctly, in Figure 11, we show the agreement between the solutions of these new equations and those in [6], to illustrate, in a qualitative way, the reliability of the formalism presented in this work.

Finally, approximate equations considering relativistic corrections have been presented and solved. As the relativistic treatment is strictly necessary for $t < t_{hor}$, where the quasi-Newtonian treatment predicted an incorrect growth of the perturbations, it is in this interval where we analyze the obtained solutions. It can be seen, qualitatively, how the application of these corrections solves the initial growth of flucuations. In this treatment it is also necessary to consider the neutrinos, whose perturbations have also been adequately obtained.

In conclusion, this work has been based on the numerical solutions of non-relativistic equa-

tions to reproduce and understand how density perturbations evolve in the first instants of the universe, as well as to deeply understand each of the physical phenomena that take place on the different constituents. In parallel, the resolution of these equations has involved the use of different numerical techniques and approximations, both numerical and theoretical, such as the Montecarlo method or the WKB approximation.

With this study, the bases of the non-relativistic analysis of density perturbations are consolidated, having verified the reliability of the equations that govern them, and, on the other hand, the relativistic treatment of these is initiated, starting with the application of approximate corrections to the previous equations.

8 Appendix

Relevant quantities

- Hubble's constant: $H_0 = 7.1638 \cdot 10^{-11}$ yr^{-1}
- Universal gravitational constant: $G = 8.93 \cdot 10^{-3}$ Mpc^{3}yr^{-2}M$_\odot^{-2}$
- Thomson's cross section: $\sigma_T = 6.9863e - 74$ Mpc^2
- Dimensionless density parameters:
  $\Omega_{0,bar} = 0.3$, $\Omega_{0,DM} = 0.26$, $\Omega_{0,\gamma} = 5.0467 \cdot 10^{-5}$, $\Omega_{0,\nu} = 3.49 \cdot 10^{-5}$
- Electron number density: $n_e(a) \simeq 4.94408 \cdot 10^{66} \chi_e(a) a^{-3} \left(\frac{\Omega_{0,bar}}{0.04}\right) \left(\frac{h_0}{0.7}\right)^2$ Mpc^3
- Ionization fraction:

$$\chi_e(a) = \begin{cases} A & a < 5.33 \cdot 10^{14} \\ A \exp -\frac{\left(\frac{a}{1-a} - B\right)^2}{2C^2} & a > 5.33 \cdot 10^{14} \end{cases}$$

  with $A = 1.079$, $B = 5.33 \cdot 10^{-4}$, $C = 2.055 \cdot 10^4$
- Horizon radius: $r_{hor}(t) = \int_0^t \frac{c}{a(t')} dt' = \int_0^t \frac{1}{a(t')^2} \sqrt{\sum_i \Omega_{i,0} a(t')^{-3(1+w)}} dt'$
- Fluctuation mass: $M(R) = 3.465 \cdot 10^{11} h^{-1} \left(\frac{R}{h^{-1}\text{Mpc}}\right)^3 \frac{\Omega_m}{0.3}$

Interpolation of functions $G(k\lambda_0)$ and $H(k\lambda_0)$

The interpolation fitting of functions $G(y)$ and $H(y)$ has been performed with `Akima1DInterpolator` from the library `scipy.interpolate` from Python.

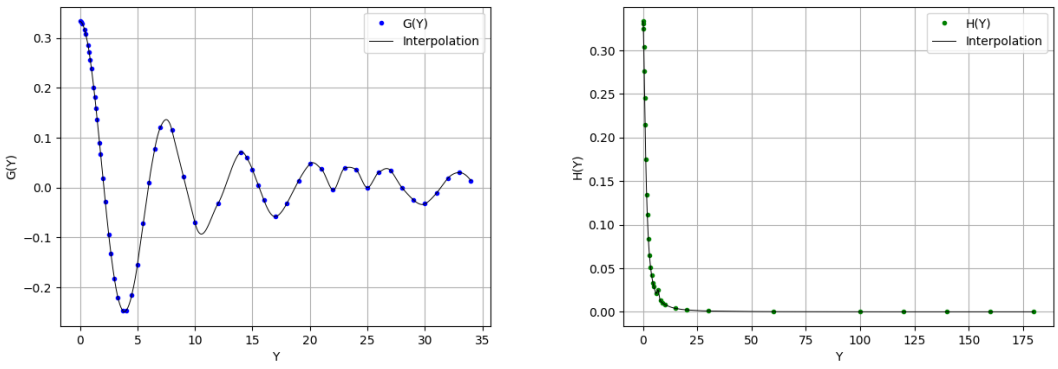

Figure 13: Interpolation fitting of functions $G(y)$ and $H(y)$.

y	$H(y)$	y	$G(y)$	y	$G(y)$
0	1/3	0	1/3	8	0.115
0.1	0.331	0.1	0.332	9	2.21e-2
0.2	0.325	0.2	0.329	10	-0.07
0.4	0.304	0.4	0.317	12	-3.23e-2
0.6	0.276	0.5	0.308	14	0.071
0.8	0.245	0.7	0.286	14.5	6.04e-2
1	0.215	0.8	0.272	15	3.62e-2
1.3	0.175	0.9	0.256	15.5	5.06e-3
1.7	0.134	1	0.239	16	-2.53e-2
2	0.112	1.2	0.201	17	-0.058
2.5	8.38e-2	1.3	0.181	18	-3.14e-2
3	6.48e-2	1.4	0.159	19	1.33e-2
3.5	5.15e-2	1.5	0.137	20	4.74e-2
4	4.18e-2	1.7	9.05e-2	21	3.71e-2
4.6	3.33e-2	1.8	6.68e-2	22	-4.53e-3
5	2.9e-2	2	1.92e-2	23	3.86e-2
6	2.13e-2	2.2	-0.0275	24	3.61e-2
7	2.48e-2	2.5	-9.36e-2	25	-2.11e-5
8	1.29e-2	2.7	-0.133	26	3.11e-2
9	1.03e-2	3	-0.183	27	3.45e-2
10	8.53e-3	3.3	-0.220	28	7.19e-5
15	4.00e-3	3.7	-0.246	29	-0.0246
20	2.31e-3	4	-0.247	30	-3.25e-2
30	1.04e-3	4.5	-0.216	31	-1.11e-2
60	2.43e-4	5	-0.154	32	1.88e-2
100	6.67e-5	5.5	-0.0723	33	3.02e-2
120	6.67e-5	6	0.0094	34	1.4e-2
140	6.67e-5	6.5	7.71e-2		
160	6.67e-5	7	0.121		
180	6.67e-5				

Table 5: Numerical values used for the interpolation fitting of functions $G(y)$ and $H(y)$.

References

[1] Sergio de Armas Rillo y Juan Betancort Rijo. "Obtention of the Baryonic and Dark Matter power spectrum using certain approximations on the equations that rule the evolution of Baryonic Acoustic Oscillations". In: (2017).

[2] Peter Coles and Francesco Lucchin. "Cosmology, The Origin and Evolution of Cosmic Structure". In: *Chichester: Wiley, —c1995* -1 (Jan. 1995).

[3] *Cosmic Background Explorer*. NASA. URL: https://lambda.gsfc.nasa.gov/product/cobe/.

[4] D. J. Fixsen. "THE TEMPERATURE OF THE COSMIC MICROWAVE BACKGROUND". In: *The Astrophysical Journal* 707.2 (Nov. 2009), pp. 916–920. ISSN: 1538-4357. DOI: 10.1088/0004-637x/707/2/916. URL: http://dx.doi.org/10.1088/0004-637X/707/2/916.

[5] Bárbara Pérez Pérez y Juan Betancort Rijo. "Estudio detallado de algunos efectos potencialmente relevantes para la determinacion de espectros de materia oscura". In: (2018).

[6] Malcolm S. Longair. *Galaxy Formation*. Astronomy and Astrophysics Library. Heidelberg, Germany: Springer, 2008. ISBN: 978-3-540-73477-2, 978-3-540-73478-9. DOI: 10.1007/978-3-540-73478-9.

[7] J. C. Mather et al. "A Preliminary Measurement of the Cosmic Microwave Background Spectrum by the Cosmic Background Explorer (COBE) Satellite". In: 354 (May 1990), p. L37. DOI: 10.1086/185717.

[8] P. J. E. Peebles. "Primeval adiabatic perturbations - Constraints from the mass distribution". In: 248 (Sept. 1981), pp. 885–897. DOI: 10.1086/159219.

[9] Planck Collaboration. "Planck 2018 results. VI. Cosmological parameters". In: *Astronomy & Astrophysics* 641 (2020), A6. DOI: 10.1051/0004-6361/201833910. URL: https://www.aanda.org/articles/aa/abs/2020/09/aa33910-18/aa33910-18.html.

[10] M. Rowan-Robinson. *Cosmology*. Oxford physics series. Clarendon Press, 1977, p. 412.

[11] S. Weinberg. *Gravitation and Cosmology: Principles and Applications of the General Theory of Relativity*. Wiley, 1972, pp. 154–68.

[12] *Wilkinson Microwave Anisotropy Probe*. NASA. URL: https://map.gsfc.nasa.gov/.